Chapter 1
Introduction

1.1 Background

Human efforts to utilize wind for energy have started in ancient times, when they used to sail the ships and boats. Later, wind energy served the mankind by providing the energy for girding mills and water pumps. During its transformation from these crude and heavy devices to today's efficient and sophisticated machines, the technology went through various phases of development [1]. In Holland, several decisive improvements were made on windmills in the 16th century, leading to a new type of mill, so called 'Dutch windmill' [1]. The era of wind electric generators began close to 1900's. The first wind turbine, specifically designed for electricity generation was constructed in Denmark in 1890. By 1910, several hundreds of such machines were supplying electrical power to the villagers in Denmark. By about 1925, the wind electric generators became commercially available in the American market. Intensive research on wind turbines started during 1950 in Germany, Denmark and USA. However, during this period, electricity generated from wind costs 8-10 times more than that of fossil fuels. But oil crisis in 1970's forced the world to think about wind power generation. In 1980s, the cost of electricity from utility-scale wind power projects was as high as 30 cents per kWh, at present, the cost of generating electricity from wind power ranges from 3 to 6 cents per kWh [1].Wind power, which has been proved as a potential source for generation of electricity with minimal environmental impact, is the fastest-growing source for electric power generation and it is expected to remain so in future. At the end of 2006, the wind installed capacity stands at over 74,223 MW which is more than 15,197 MW from the capacity in 2005 [1, 27]. World Wind Energy Association (WWEA) expects 160 GW to be installed worldwide by 2010. Despite constraints facing supply chains for wind turbines, the annual market for wind continued to increase at the staggering rate of 32%following the 2005 record year, in which the market grew by 41%. In terms of economic value, the wind energy sector has now become firmly installed as one of the important players in the energy markets [1, 27]. Harnessing wind energy for electric power generation is an area of research interest and at present, the emphasis is given to the cost effective utilization of this energy resource for quality and reliable power supply.

1.2 Aerodynamic Conversion

The kinetic energy available in the wind is converted into mechanical energy by the rotor blades of the wind turbine. For steady-state calculations of the mechanical power from a wind turbine, the so called *Cp* (*λ, β*)-curve can be used [2]. In general, the relation between wind speed and mechanical power extracted from the wind can be given as

$$P_m = \frac{\rho}{2} A C_p(\lambda, \beta) v_w^{\,3} \qquad 1.1$$

Where, *Pm* is the power extracted from the wind; ρ is the air density; *Cp* is the performance coefficient or power coefficient; λ is the tip-speed ratio; $A_r = 2\Pi R$ is the area covered by the wind turbine rotor blades; *R* is the radius of the rotor; v_w denotes the wind speed; and β is the blade pitch angle. The tip-speed ration λ is defined as

$$\lambda = \frac{\omega_r R}{v_w} \qquad 1.2$$

Where, $\omega_r = P/2*\omega_m$ is the electrical speed (elec. rad/s), P is the number of pole DFIG, and ω_m is the mechanical speed of the rotor (mech. rad/s).By combining Eq. (2.1) and (2.2), we can see that

$$P_m = \frac{\rho}{2} \pi * R^5 C_p \frac{\omega_r^{\,3}}{\lambda^3} \qquad 1.3$$

At high wind speeds it is necessary to limit the input power to the wind turbine, i.e., aerodynamic power control. There are three major ways of performing the aerodynamic power control, i.e., by stall, pitch, or active stall control. Stall control implies that the blades are designed to stall in high wind speeds and no pitch mechanism is thus required.

Pitch control is the most common method of controlling the aerodynamic power generated by a turbine rotor, for newer larger wind turbines. Almost all variable-speed wind turbines use pitch control [3]. Below rated wind speed the turbine should produce as much power as possible, i.e., using a pitch angle that maximizes the energy capture. Above rated wind speed, the pitch angle is controlled in such a way that the aerodynamic power is at its rated. In order to limit the aerodynamic power, at

high wind speeds, the pitch angle is controlled to decrease the angle of attack, i.e., the angle between the chord line of the blade and the relative wind direction. It is also possible to increase the angle of attack towards stall in order to limit the aerodynamic power. This method can be used to fine-tune the power level at high wind speeds for fixed-speed wind turbines. This control method is known as "*active stall"* or "*combi stall"*.

1.2 Wind energy conversion systems (WESC)

Wind turbines can operate either at fixed speed (actually within a speed range about 1%) or at variable speed. For fixed-speed wind turbines, the generator (induction generator) is directly connected to the grid. A soft starter is normally used in order to reduce the inrush current during start-up. Also a reactive power compensator is needed to reduce (almost eliminate) the reactive power demand from the wind generators. Since the speed is almost fixed to the grid frequency, and certainly not controllable, it is not possible to store the turbulence of the wind in form of rotational energy. Therefore, for a fixed-speed system the turbulence of the wind will result in power variations, and thus affect the power quality of the grid. The advantage of a fixed speed turbine is that it is relatively simple and therefore the investment cost tends to be slightly lower. These turbines have to be more mechanically robust than other designs, because of the higher structural loads involved [1, 3]. With a fixed speed WECS, it may be necessary to use aerodynamic control of the blades to optimize the whole system performance, thus introducing additional control systems, complexities, and costs. These turbines have to be more mechanically robust than other designs, because of the higher structural loads involved. For a variable-speed wind turbine, the generator is controlled by power electronic equipment, which makes it possible to control the rotor speed. The power fluctuations caused by wind variations can be more or less absorbed by changing the rotor speed and thus power variations originating from the wind conversion and the drive train can be reduced. Hence, the power quality impact caused by the wind turbine can be Improved compared to a fixed-speed turbine. Another advantage is that variable speed turbines also allow the grid voltage to be controlled, as the reactive

power generation can be varied. The rotational speed of a wind turbine is fairly low and must therefore be adjusted to the electrical frequency. The major drawbacks of variable speed systems are that the built-in power electronics are sensitive to voltage dips caused by faults and/or switching [1, 3].

1.4 Generator Configurations for Grid Connected systems

Several kinds of generator technologies have been developed and are in use today. In this section a short overview of the various generator topologies that are suitable for fixed and variable speed wind turbines, have been presented [4].

1.4.1 Fixed speed wind speed systems

Induction generator is the prevalent choice for fixed speed wind energy systems because of its simplicity, robustness and relatively low cost. In fixed-speed wind turbine the induction generator is directly connected to the electrical grid as shown in Fig. 1.1.The rotor speed of the fixed-speed wind turbine is determined by the gearbox and the number of poles of the generator. Often the fixed-speed wind turbine systems are provided with two fixed speeds. This is accomplished by using two generators with different ratings and pole pairs, or it can be a generator with two windings having different ratings and pole pairs. This will increases the aerodynamic capture as well as reduces the magnetizing losses of generator at low wind speeds. When induction machines are operated using vector-control techniques, fast dynamic response and accurate torque control are obtained [1].

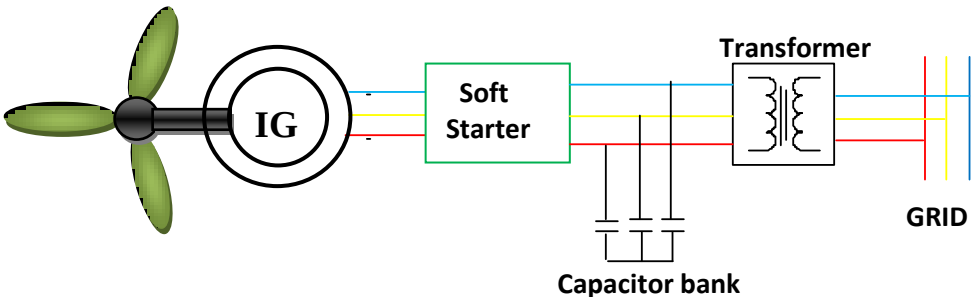

Fig. 1.1 Schematic of fixed speed wind turbine with IG, connected to grid

1.4.2 Variable speed wind systems

For variable speed wind systems, the generators can be used are Induction Generator (IG), Synchronous or Permanent Magnet Synchronous generator (SG or PMSG), and Doubly Fed Induction Generator (DFIG).

1.4.2.1 Variable Speed wind turbine with IG or SG/PMSG

A variable speed wind turbine equipped with IG or SG/PMSG, connected to the grid through a converter, is shown in Fig. 1.2.

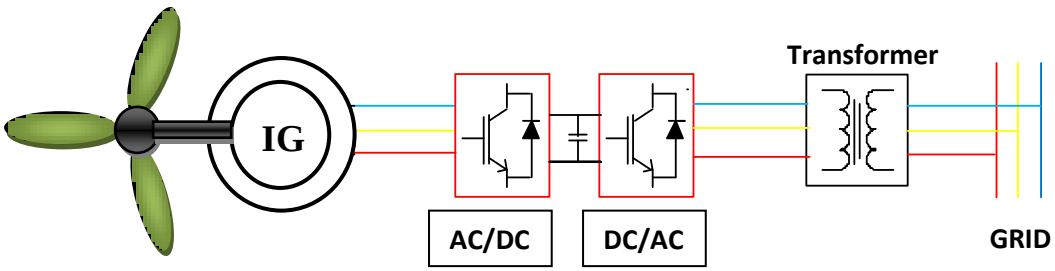

Fig. 1.2 Schematic of variable speed wind turbine with IG or SG, connected to grid

The induction generator could be either cage-bar rotor or wound rotor type. The gearbox is designed so that maximum rotor speed corresponds to rated speed of the generator. Synchronous generators or permanent-magnet synchronous generators can be designed with multiple poles, so that there is no need for gearbox. The power electronic equipment has to be designed for the full power rating of the generator. Future of wind turbine technology lies in PMSG. With the permanent magnet, high power densities can be achieved in a less space. Hence, the generators become much more compact with high efficiencies. Notable advantage is absence of gearbox and its acoustic noise. The main limitation for PMSG is the high cost of the materials for the

Magnet. Also, generators with permanent magnet excitation have a poor power factor and can be compensated by inverter technology. The cost of power converter can be high due to its large size and also the losses in the converter are large. One major advantage with this system is it's well developed and robust in control.

1.4.2.2 Variable speed wind turbine with DFIG (conventional DFIG system

For variable-speed wind systems with limited slip, e.g. ±30%, the DFIG can be an interesting solution. The major advantage of the doubly-fed induction generator, which has made it popular, is that the power electronic equipment only has to handle a fraction (20–30%) of the total system power. This means that the losses in the power electronic equipment can be reduced in comparison to power electronic equipment that has to handle the total system power as for a direct-driven synchronous generator, apart from the cost saving of using a smaller converter. In addition, the cost of the converter becomes lower. The schematic of DFIG with stator circuit connected to the grid while the rotor circuit is connected to a converter via slip rings is as shown in Fig. 1.3. Doubly-fed induction generators (DFIG) are provided with three phase windings on the rotor and on the stator. They may be supplied with energy at both rotor and stator terminals.

The back-to-back converter consists of two converters, i.e., rotor-Side Converter **(RSC)** and Grid-Side Converter **(GSC).** Between the two converters a dc-link capacitor is placed, as energy storage, in order to keep the voltage variations (or ripple) in the dc-link voltage small. With the machine-side converter it is possible to control the torque or the speed of DFIG and also the power factor at the stator terminals, while the main objective for the Grid-side converter is to keep the dc-link voltage constant.

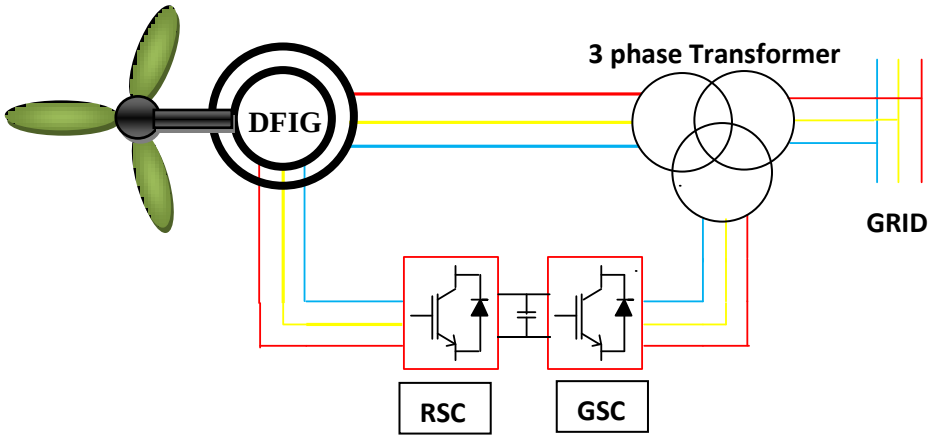

Fig. 1.3 Schematic of Conventional DFIG wind system

The speed–torque characteristics of the DFIG system can be seen in Fig. 2.2. As also seen in the figure, the DFIG can operate both in motor and generator operation with a rotor-speed range of ± $\Delta\omega_r$ max around the synchronous speed, ω_s.

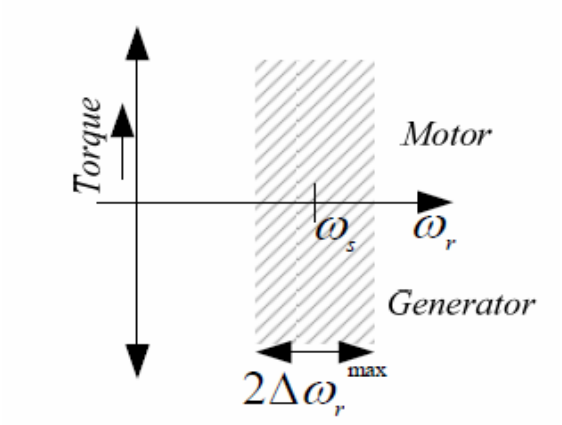

Fig. 1.4 Speed–Torque characteristics of DFIG

1.5 State of the Art

A detailed comparison of various wind turbine topologies has been presented in [1, 3, 4]. In [5] a comparison of energy captured by various wind energy systems has been given. According to [5] the energy capture can be significantly increased by using a DFIG and the energy capture of a DFIG system is increased by over 20% with respect to a variable-speed system using a cage-bar induction machine. Today, doubly-fed induction generators are commonly used for the large wind power generation. The DFIG modelling has been given in [19, 10].The major advantage of the doubly-fed induction generator, which has made it popular, is that the power electronic equipment only has to handle a fraction (20–30%) of the total system power [1,3, 21]. Control of the DFIG is more complicated than the control of a standard induction machine. In order to control the DFIG the rotor circuit is controlled by a power electronic converter while the stator circuit of DFIG is directly excited from the PCC voltage. One common way of controlling the rotor current is by means of field-oriented (vector) decoupling control [6, 16, 20, 24]. The strength of the conventional DFIG in power processing, namely direct connection of the stator windings to the PCC, turns out to be a source of weakness in regards to tolerating PCC voltage disturbances [7, 9, 14]. As the penetration of large scale wind turbines into the electric power grid continues to increase, the response of wind turbines to grid disturbances is an important issue Therefore, it is important to study the effects of various voltage sags and grid faults on the grid connected DFIG wind systems. New grid codes will require WTs and wind farms to ride through voltage sags, meaning that normal power production should be re-initiated once the nominal grid voltage has been recovered [8, 18].Many authors have explored the performance of DFIG system through time domain simulation studies [7, 9, 14, 15]. Time-domain studies offer a direct appreciation of the dynamic behaviour in terms of visual clarity. However, they are not able to identify and quantify the cause and nature of interactions and problems. This complementary information can be obtained with Eigen value studies [10, 11, 23].

A possibility to limit the high current in the rotor in order to protect the converter and to provide a bypass for this current via a set of resistors that are connected to the rotor windings so called crowbar [8, 9] during the faults without disconnecting the turbine from the grid. During period of operation of crowbar the control action of the converter is trimmed to shut down and allow the DFIG to operate as a conventional slip-ring induction machine.

1.6 Thesis Organization

The thesis has been organized into five chapters. The present chapter introduces very briefly, the various wind energy schemes and some of the technical challenges with the inter connection of grid. It presents the relevant state of art survey and sets the motivation behind the work carried out in the thesis.

Chapter-2, describes the literature survey of the project.

Chapter-3, describes the general modelling of conventional DFIG system and its control schemes.

Chapter-4, introduces two new control techniques to control the stator voltage and frequency, and to extract the maximum power from the DFIG. And there controller designs to improve the performance during unhealthy conditions.

Chapter-5 presents conclusions and future scope of the project

CHAPTER 2
LITERATURE SURVEY

2.1 GENERAL

The last few years have seen the emergence of wind generation as the leading source of renewable energy in the power industry. Wind farms totalling hundreds, even thousands, of MW are now being considered. “Making room” for this new type of generation in electric network poses significant challenges on a wide range of issues. this thesis addresses one of those issues, objective of this work is to study various control techniques of DFIG for wind energy conversion systems (WECS) and the modelling of wind energy conversion system with doubly-fed induction generator (DFIG) for variable speed wind energy systems. A substantial literature available in this field is vast and covers the whole range of control techniques for designing and modelling of WECS. A brief literature review on these topics is given here.

2.2 LITERATURE REVIEW

In recent years, wind energy has become one of the most important and promising sources of renewable energy, the evolution of technology related to wind systems leaded to the development of a generation of variable speed wind turbines. Doubly-fed induction generator (DFIG) is one of the most popular wind turbines which include an induction generator with slip ring, a partial scale power electronic converter and a common DC-link capacitor. The power electronic converters are two back-back (AC/DC/AC) voltage source fed converters placed in between rotor and grid circuit.

The power electronic converters are used to synchronize the variable speed induction generator with the grid by controlling switching sequence of gating pulses, many different control algorithms applied to control the DFIG for wind energy applications. Rotor side converter is responsible for synchronization of GFIG with grid, both rotor and stator side converters handle quantities (slip and grid frequency, respectively), they are controlled by vector controlled techniques [26]. A typical implementation of such control concepts is detailed in [27], vector control is based on the concept of developing a rotating reference frame based on an ac flux or voltage and projecting

currents on such a rotating frame. Such projections are usually referred to as the d-q components of their respective currents. With a suitable choice of reference frames, the ac quantities appear as dc quantities in the steady state. For flux based rotating frames, changes in the d-axis component will lead to reactive power(voltage)changes, changes in the q-axis component of current will vary the active power (frequency)changes. In voltage-based rotating frames (and thus 90deg.ahead of flux-based frames) the effect is the opposite. The d-q components are normally driven to reference levels via only proportional (**P**) controllers, or both proportional + integral (**PI**) controllers.

In DFIG the reference levels are in turn typically set by controllers such as:

- An electrical torque controller driving the rotor-side converter i_q controller(flux based controller)
- Capacitor voltage controller driving the stator-side converter i_d controller(voltage based controller)
- Ac voltage controllers driving the i_d and i_q controllers on both rotor and stator side converters.

2.2.1 CONTROL TECHNIQUES OF DFIG

Stator voltage oriented (SVO) or stator flux oriented (SFO)vector control [28-30] and direct power control (DPC) [31-32] are the two most popular control strategies for the grid-side and rotor side converters in a DFIG system. Theoretically, the vector control provides fault ride-through capability under both balanced [28] and unbalanced grid-fault conditions [29] and has been undergoing significant development. But the complexity of control structure, especially under unbalanced grid-fault conditions, is the main drawback which boosts the demands on the hardware and the robustness of the control system. The conventional direct power control simply selects the switching states of the converter from an optimal switching table, based on the instantaneous errors between active and reactive powers and their references. However, the conventional DPC has several drawbacks which make it difficult to be applied in the DFIG-based wind power generation system. For example, the rotor voltages generated by a fixed and discrete switching table cannot satisfy the control precision of the active and reactive powers during maximum wind-energy capturing.

[30]Furthermore, the electromagnetic torque vibration caused by the traditional DPC is much more significant than that in the vector control with the same sampling frequency. Moreover, the conventional DPC complicates the AC filter design because of its variable switching frequency. To overcome these drawbacks, several modified strategies have been reported [34-36]. In [34], the authors developed a modified DPC referred to as the output regulation subspaces based DPC (DPC-ORS), which was implemented via rotating the voltage vector with a pre-calculated angle for the purpose of refining the selection of control vector. In [35], though the variation in duty cycle of voltage vector within each sampling period which in turn was generated from a PI controller minimizes electromagnetic torque fluctuation. But this controller makes the system structure more complex. A simple and more effective method was proposed by calculating the required rotor controlling voltage within each sampling period directly based on the estimated stator flux, active and reactive powers and their errors [36]. Meanwhile, a constant switching frequency was together been achieved by the space vector modulation (SVM) technique. However this method still encounters some problems such as over-current and electromagnetic torque vibration under grid voltage dips. To overcome the above problems, the authors proposed three selectable DPC strategies for the wind turbine driven DFIG system based on the detailed mathematical analysis [37]. These strategies are controlling the DFIG rotor flux, rotor current and electromagnetic torque but conventional direct power control has several draw backs like it purely depends on the system parameters, stator rotor resistance inductance, and mutual inductance, ect thus, the performance is degraded when the actual machine parameters differ from those values used in the control system. A new technique based on vector control a decoupled active and reactive power was reported where both the active and reactive powers are controlled independently by controlling the rotor d-axis, q-axis currents [38].

A stand alone operation of DFIG, where the load voltage is maintained at constant frequency and its magnitude is regulated through control of the stator flux of the generator is reported in literature, Where an auxiliary load is connected in parallel with the main load, and the auxiliary power is controlled to allow the DFIG to track the optimal wind turbine speed for maximum energy capture from the wind. In modification to above an indirect stator-orientated vector control scheme is used to control the DFIG and these results in constant load voltage and frequency even under variations in both load and wind speed [39]. In this method, the load on the generator

is maintained constant using an auxiliary load, to generate voltage at constant frequency. The control scheme is load dependent, but there is a gross wastage of the generated power. Need is felt for a better control strategy which is independent of load and parametric variations of the machine and the system. The control scheme should be fast enough to control the oscillations.

The repeated control techniques are based on voltage control, the scheme based on current control has reported 10 times faster and stable operation than the voltage control technique [26], it is also reported that dynamics of current controllers in DFIG are much faster than the electromechanical dynamics of interest during transient stability simulations. Since the current control method does not require any knowledge of load parameters, it may not require any auxiliary load etc.

2.3Identified Research Areas

The study of existing literature has revealed the following research areas for further investigations.

- All the reported control strategies are open loop. Design of a simple fast closed loop voltage and frequency with current control strategy, which is independent of system parameters, load variations is very much in need.

- Design of control scheme and modelling techniques to extract the maximum power tracking from the wind turbine for the rotor-side converter it also needed.
- A simple and fast control algorithm is required to extract the maximum power tracking from the wind energy. Design of control scheme and modelling techniques to avoid the problems of voltage fluctuation and harmonic distortion caused due to grid connected renewable energy sources.

- Development of hybrid systems combining wind energy conversion system and other renewable energy sources known as diesel generators, small hydro, fuel cell, photovoltaic cell, battery energy storage etc, with grid connected without grid connected

2.4 CONCLUSIONS

A substantial work has been carried out in the field of wind energy conversion system (WECS) by employing synchronous and asynchronous generators with various controlling techniques. This is reported by the various researchers. The technology of WECS has matured enough to the implementation stage and some of the prototypes are performing at the load end or distribution level. There is still significant scope of further research work and investigations are needed in terms of new, simple and improved control algorithms suitable for WECS with different types of hybrid systems.

Chapter 3
MODELLING OF DFIG

3.1 General

Today, doubly fed induction generators are more increasingly used for the large wind power generation. Since their power electronic equipment only has to handle a fraction (20–30%) of the total system power. This means that the losses in the power electronic equipment can be reduced in comparison to power electronic equipment that has to handle the full system power as for a direct driven induction generator, apart from overall cost effectiveness. The semiconductor AC/DC and then DC/AC conversion is used to control the bidirectional power delivered from/to the rotor circuit to/from the grid.

In this chapter, modelling of DFIG and its rotor and grid side converter controller structures has been presented. As modelling of the system provide valuable information of the DFIG properties, limitations and control options, a model of of grid connected conventional DFIG has been performed.

3.2 Basic operating principle of DFIG

The doubly-fed induction generator (DFIG) is a 'special' variable speed induction machine and is widely used as modern large wind turbine generators. It is a standard, wound rotor induction machine with its stator windings directly connected to the grid and its rotor windings connected to the grid through an AC/DC/AC **PWM** converter. The **AC/DC/AC** converter normally consists of a rotor-side converter and a grid-side converter, By means of the bi-directional converter in the rotor circuit, the DFIG is able to work as a generator in both sub-synchronous (positive slip s>0) and over-synchronous (negative slip s<0) operating area. Depending on the operating condition of the drive, the power is fed in or out of the rotor (**P_{rotor}<0)**: it is flowing from the grid via the converter to the rotor in sub-synchronous mode or vice versa (**P_{rotor}**>0) in over-synchronous mode, In both cases (sub-synchronous and over-synchronous) the stator is feeding energy to the grid (**P_{stator}**>0) []

3.3 Doubly fed induction generator for wind system

For variable speed systems with limited variable-speed range, e.g. ±30% of synchronous speed, the DFIG is reported to be an interesting solution. A detailed representation of DFIG with its back to back converters is depicted in Fig 3.1. The back-to-back converter consists of two converters, i.e., rotor-side converter (RSC) and grid-side converter (GSC), connected "back-to-back." Between the two converters a DC-link capacitor is placed. With the rotor-side converter it is possible to control the torque or the speed of the DFIG. Doubly fed induction machines can be operated as a generator as well as a motor in both sub-synchronous and super synchronous speeds using the rotor side converter control. Only the two generating modes at sub-synchronous and super synchronous speeds are of interest for wind power generation.

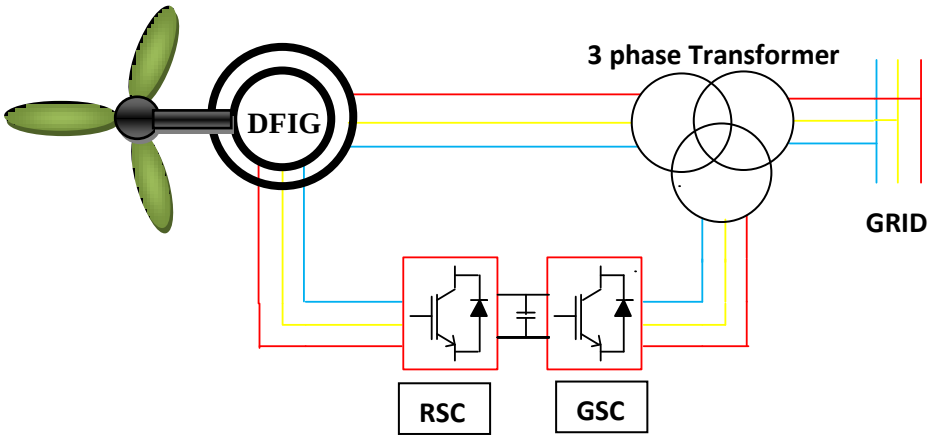

Fig. 3.1 Schematic of Conventional DFIG wind system

The speed–torque characteristics of the DFIG system can be seen in Fig. 3.2. As also seen in the figure, the DFIG can operate both in motor and generator operation with a rotor-speed range of $\pm \Delta\omega_r^{max}$ around the synchronous speed, ω_s.

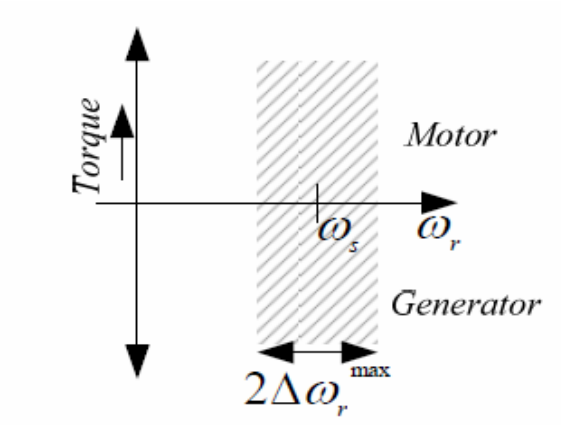

Fig. 3.2 Speed–Torque characteristics of DFIG

3.3 Equivalent Circuit of DFIG

The equivalent circuit of the doubly-fed induction generator, including the magnetizing losses, can be seen in Fig. 3.3. This equivalent circuit is valid for steady state calculations. The DFIG under study is Y connected and its equivalent is given below.

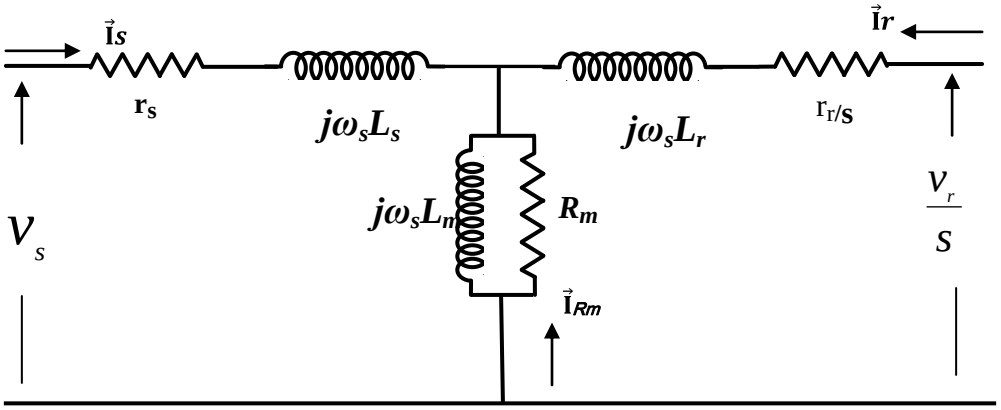

Fig. 3.3 Equivalent circuit of doubly fed induction generator

If the rotor voltage, V_r in Fig. 3.3., is short circuited, the equivalent circuit for the DFIG becomes the equivalent circuit for an ordinary cage-bar induction machine. The conventional motor direction of stator current I_s and rotor current I_r is adopted. On the Stator side, r_s and ($j\omega_s L_s$) are the resistance and leakage reactance of stator

winding. On the rotor side, r_r and ($j\omega_s L_r$) are the resistance and leakage reactance of the rotor winding. The mutual reactance is (jωsM). When the rotor rotates at angular velocity of ω_r electrical rad/s, the rotor resistance, r_r is modified as r_r/s where, s = (1 − ω_r/ω_s) is the slip. The rotor-side VSC injects balanced three-phase currents (i_{ra}, i_{rb}, i_{rc}) at slip frequency "sω_s", voltage magnitude 'V_r' and voltage angle 'δ'. Because Fig. 2.3. is based on the stator-side frequency 'ω_s', the VSC voltage phasor $V_r = V_r|\underline{\delta}$ representing (V_{ra},V_{rb}, V_{rc}) has also to be divided by the slip 's' resulting in the equivalent rotor voltage ($\frac{V_r|\underline{\delta}}{s}$) . Applying Kirchhoff's voltage law to the equivalent circuit shown in Fig. 3.3.

$$\overline{V_s} = r_s \bar{I}_s + j\omega_s L_s \overline{I_s} + j\omega_s L_m(\overline{I_s} + \overline{I_m} + \overline{I_{Rm}}) \quad 3.1$$

$$\frac{\overline{V_r}}{s} = \frac{r_r}{s}\overline{I_r} + j\omega_s L_r \overline{I_r} + j\omega_s L_m(\overline{I_s} + \overline{I_r} + \overline{I_{Rm}}) \quad 3.2$$

$$0 = R_m \overline{I_{Rm}} + j\omega_s L_m(\overline{I_s} + \overline{I_r} + \overline{I_{Rm}}) \quad 3.3$$

Where, V_s is the stator voltage; I_{Rm} is the magnetizing resistance current. The air-gap flux, stator flux and rotor flux are defined as

$$\overline{\psi_m} = L_m(\overline{I_s} + \overline{I_r} + \overline{I_{Rm}}) \quad 3.4$$

$$\overline{\psi_s} = L_s\overline{I_s} + L_m(\overline{I_s} + \overline{I_r} + \overline{I_{Rm}}) = L_s\overline{I_s} + \overline{\psi_m} \quad 3.5$$

$$\overline{\psi_r} = L_r\overline{I_r} + L_m(\overline{I_s} + \overline{I_r} + \overline{I_{Rm}}) = L_r\overline{I_r} + \overline{\psi_m} \quad 3.6$$

The equations describing the equivalent circuit, i.e., Eqs. (3.1) – (3.3), can be rewritten as

$$\overline{V_s} = r_s \bar{I}_s + j\omega_s \overline{\psi_r} \quad 3.7$$

$$\frac{\overline{V_r}}{s} = \frac{r_r}{s}\overline{I_r} + j\omega_s \overline{\psi_r} \quad 3.8$$

$$0 = R_m \overline{I_{rm}} + j\omega_s \overline{\psi_m} \quad 3.9$$

3.4 power flow equations

In order to investigate the power flow of the conventional DFIG system the apparent power that is fed to the DFIG via the stator and rotor circuit has to be determined. The stator apparent power S_s and rotor apparent power S_r can be given as

$$\overline{S_s} = 3\overline{V_s}\,\overline{I_s}^{*} = 3\left|\overline{I_s}\right|^2 r_s + 3j\omega_s L_s \left|\overline{I_s}\right|^2 + 3j\omega_s \overline{\psi_m}\left|\overline{I_s}\right|^{*} \quad 3.10$$

$$\overline{S_r} = 3\overline{V_r}\,\overline{I_r}^{*} = 3\left|\overline{I_r}\right|^2 r_r + 3j\omega_s L_r \left|\overline{I_r}\right|^2 + 3j\omega_s s\overline{\psi_m}\left|\overline{I_r}\right|^{*} \quad 3.11$$

This can be written as

$$\overline{S_s} = 3\left|\overline{I_s}\right|^2 r_s + 3j\omega_s L_s \left|\overline{I_s}\right|^2 + 3j\omega_s \frac{\overline{\psi_m}^{\,2}}{L_m} + 3R_m \left|\overline{I_{Rm}}\right|^2 - 3j\omega_s \overline{\psi_m}\left|\overline{I_r}\right|^{*} \quad 3.12$$

$$\overline{S_r} = 3\left|\overline{I_r}\right|^2 r + 3j\omega_s L_r \left|\overline{I_r}\right|^2 + 3j\omega_s \overline{\psi_m}\left|\overline{I_r}\right|^{*} \quad 3.13$$

Now the stator and rotor power can be determined as

$$P_s = \mathrm{Re}\left[\overline{S_s}\right] = 3\left|\overline{I_s}\right|^2 r_s + 3R_m \left|\overline{I_{Rm}}\right|^2 + 3\omega_s \overline{I_m}\left[\overline{\psi_m}\,\overline{I_r}^{*}\right] \approx 3\omega_s \overline{I_m}\left[\overline{\psi_m}\,\overline{I_r}^{*}\right] \quad 3.14$$

$$P_r = \mathrm{Re}\left[\overline{S_r}\right] = 3\left|\overline{I_r}\right|^2 r_r - 3\omega_s s\left[\overline{\psi_m}\,\overline{I_r}^{*}\right] \approx -3\omega_s s\overline{I_m}\left[\overline{\psi_m}\,\overline{I_r}^{*}\right] \quad 3.15$$

The resistive losses and the magnetizing losses have been neglected. From the above equations the mechanical power produced by the DFIG can be determined as the sum of the stator and rotor power as

$$P_m = P_s + P_r = 3\omega_s \overline{I_m}\left[\overline{\psi_m}\,\overline{I_r}^{*}\right] - 3\omega_s s\overline{I_m}\left[\overline{\psi_m}\,\overline{I_r}^{*}\right] = 3\omega_r \overline{I_m}\left[\overline{\psi_m}\,\overline{I_r}^{*}\right] \quad 3.16$$

The electromechanical torque produced by DFIG is given by dividing the mechanical power produced P_m with mechanical rotor speed, $\omega_m = \frac{\omega_r}{np}$.

$$T_e = 3n_p \overline{I_m}\left[\overline{\psi_m}\,\overline{I_r}^{*}\right] \quad 3.17$$

And

$$P_s \approx \frac{P_m}{(1-s)} \;\&\; P_r = \frac{-sP_m}{(1-s)} \quad 3.18$$

The power flow of a "loss less" DFIG system can be as shown in Fig. 2.4. In the figure it can be seen how the mechanical power divides between the stator and rotor circuits and that it is dependent on the slip. The rotor power is approximately minus the slip times stator power: $p_r \approx -sp_s$.

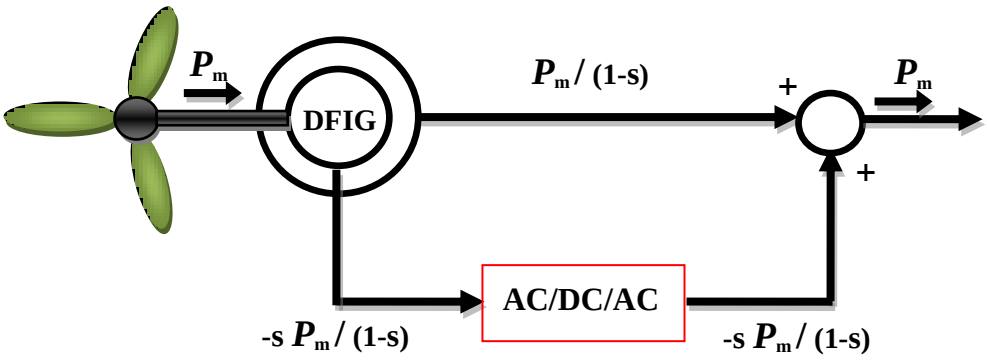

Fig. 3.4 Power flow of a "lossless" DFIG system

3.4 Modeling of DFIG

Modelling based on equivalent circuit approach is present in the sub sections. Since the rotor is operating at slip frequency and stator circuit at line frequency the analysis and control is resorted to arbitrary d-q frames.

3.4.1 T representation: Approximate Model

The vector control techniques allow de-coupled control of active and reactive power. These techniques are based on the concept of d-q controlling in different reference frames, where the current and the voltage are discomposed into distinct components related to the frequency and voltage. In below shown fig an equivalent circuit of the DFIG can be see

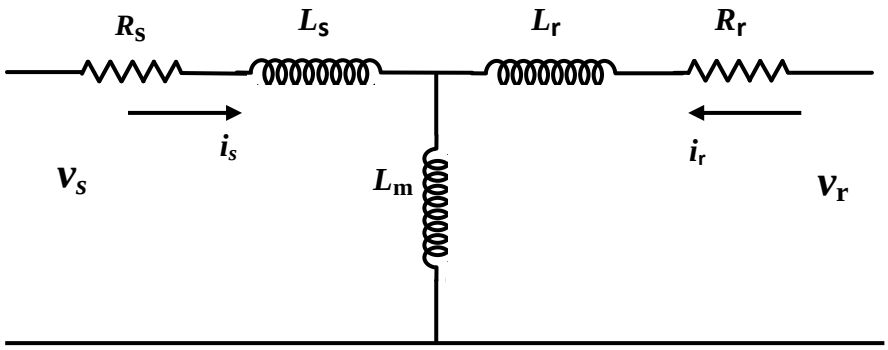

Fig 3.5 T representation of the DFIG in stator coordinates

This model is described by the fallowing space vector equations in synchronous coordinates as [ ]

$$v_{sd} = R_s i_{sd} + \frac{d}{dt}\psi_{sd} - \omega_s \psi_{sq} \quad 3.19$$

$$v_{sq} = R_s i_{sq} + \frac{d}{dt}\psi_{sq} + \omega_s \psi_{sd} \quad 3.20$$

$$v_{rd} = R_r i_{rd} + \frac{d}{dt}\psi_{rd} - \omega_{sl} \psi_{rq} \quad 3.21$$

$$v_{rq} = R_r i_{rq} + \frac{d}{dt}\psi_{rq} + \omega_r \psi_{rd} \quad 3.22$$

$$\psi_{sd} = L_s i_{sd} + L_m i_{rd} \quad 3.23$$

$$\psi_{sq} = L_s i_q + L_m i_{rq} \quad 3.24$$

$$\psi_{rd} = L_m i_{sd} + L_r i_{rd} \quad 3.25$$

$$\psi_{rq} = L_m i_{sq} + L_r i_{rq} \quad 3.26$$

When the d-q reference frame synchronous coordinates was oriented along with the stator flux of the DFIG, the V_{sq} is zero and the amplitude of the supply voltage V_{sd} is constant v_m the active and reactive power can be written as

$$P_s = v_m \frac{L_m i_{rd}}{L_s} \quad 3.27$$

$$Q_s = v_m \frac{L_m i_{rq} + \psi_s}{L_s} \quad 3.28$$

From the above two equations (3.93.10) We can see that the active and reactive power can be indirectly controlled via control i_{rd} and i_{rq} which the direct axis current i_{rd} was used to regulate the active power and the quadrate axis current component i_{rq} was used to regulate the reactive power.

3.4.2 Modeling in d-q reference frame

Consider an arbitrary dq reference frame rotating at an arbitrary speed 'ω' rad/s with respect to the stator of DFIG. The DFIG with its stator, rotor rotating at speed 'ω_r 'rad/s and arbitrary reference frame rotating at speed 'ω' rad/s is shown in Fig**.** 3.6.Any quantity in 'abc' reference frame can be converted into dq reference frame by using transformation matrix. For easier control, the three phase variables are transformed into 'dq' variables. In matrix notation, we have

$$\overline{X_{dq0}} = c\overline{X_{abc}} \qquad 3.29$$

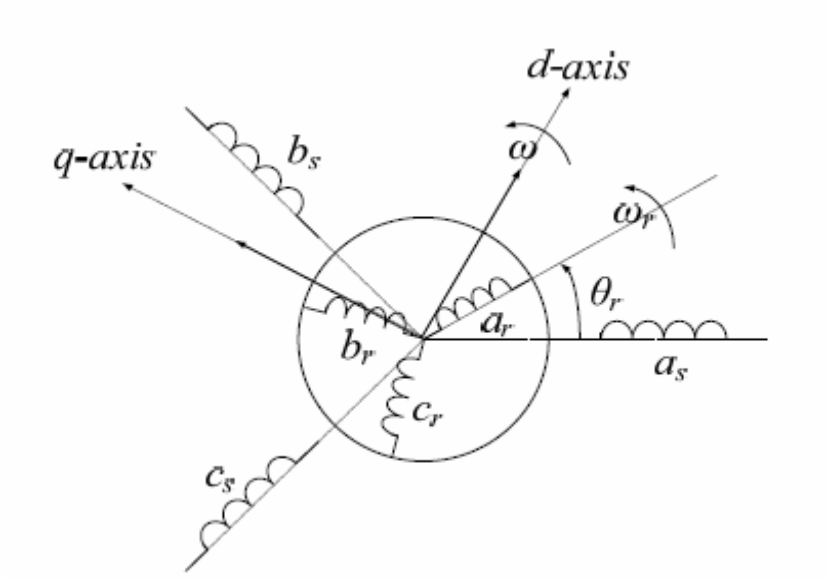

Fig. 3.6 DFIG with arbitrary reference frame rotating at 'ω' rad/s

Where, '*C*' is the 'abc' to dq transformation matrix;

$\overline{X_{dq0}} = \left[X_d X_q X_0\right]$ and $\overline{X_{abc}} = \left[X_a X_b X_c\right]$

$$c = \frac{2}{3}\begin{pmatrix} \cos(\theta) & \cos(\theta - \frac{2\pi}{3}) & \cos(\theta + \frac{2\pi}{3}) \\ \sin(\theta) & \sin(\theta - \frac{2\pi}{3}) & \sin(\theta + \frac{2\pi}{3}) \\ \frac{1}{2} & \frac{1}{2} & \frac{1}{2} \end{pmatrix} \qquad 3.30$$

Where, $\theta = (\omega t)$;

The transformation of stator voltage in 'abc' reference frame to 'dq0' reference results in

$$\overline{V_{dq0s}} = R_s \overline{I_{dq0s}} + p\overline{\psi_{dq0s}} + \omega\overline{\psi_{dq0s}} \quad 3.31$$

Where, ω matrix is represented as;

$$\omega = \begin{pmatrix} 0 & -\omega & 0 \\ \omega & 0 & 0 \\ 0 & 0 & 0 \end{pmatrix} \quad 3.32$$

Where, ψ_{dqos} is the stator flux linkages in 'dq' reference frame and it is obtained by transforming ψ_{abcs} into ψdqos using the below relation.

$$\overline{\psi_{dq0s}} = c_s L_{ss} c_s^{-1} \overline{i_{dq0s}} + c_s L_{sr} c_r^{-1} \overline{i_{dq0r}} \quad 3.33$$

where, *Cs = C; Cr* is obtained by replacing 'θ' in *C* by 'θ-θ_r', as the rotor is rotating with a relative speed of 'ω-ω_r', with respect to 'dq' reference frame.

The terms '$C_sL_{ss}C_s^{-1}$' and '$C_sL_{sr}C_r^{-1}$' are given as

$$C_s L_{ss} C_s^{-1} = \begin{pmatrix} L_{ls} + L_m & 0 & 0 \\ 0 & L_{ls} + L_m & 0 \\ 0 & 0 & L_{ls} \end{pmatrix} \quad 3.34$$

Where, Lm = 3/2 Lms and similarly

$$C_s L_{sr} C_s^{-1} = \begin{pmatrix} L_m & 0 & 0 \\ 0 & L_m & 0 \\ 0 & 0 & L_{ls} \end{pmatrix} \quad 3.35$$

The stator d and q axis flux linkages are obtained by substituting above matrices'CsLssCs-1' and 'CsLsrCr-1' in Eq. (3.34). The stator d-axis and q-axis flux linkages are obtained as:

$$\psi_{ds} = (L_{ls} + L_m) i_{ds} + L_m i_{dr} \quad 3.36$$

$$\psi_{dr} = (L_{ls} + L_m) i_{qs} + L_m i_{dr} \quad 3.37$$

From Eq. (2.51) the stator voltages on dq axes are given as

$$v_{ds} = r_s i_{ds} + p\psi_{ds} - \omega\psi_{qs} \quad 3.38$$

$$v_{qs} = r_s i_{qs} + p\psi_{qs} + \omega\psi_{ds} \quad 3.39$$

Similarly, the rotor flux linkages and rotor voltage equations in 'abc' reference frame can be transferred to dq reference frame and they are given as

$$v_{dr} = r_r i_{dr} + p\psi_{dr} - (\omega - \omega_r)\psi_{qr} \quad 3.40$$

$$v_{qr} = r_r i_{qr} + p\psi_{qr} - (\omega - \omega_r)\psi_{dr} \quad 3.41$$

$$\psi_{dr} = (L_{lr} + L_m)i_{dr} + L_m i_{ds} \quad 3.42$$

$$\psi_{qr} = (L_{lr} + L_m)i_{qr} + L_m i_{qs} \quad 3.43$$

The above rotor voltage equations in 'dq' reference frame are obtained by replacing ω in the stator voltage equation by ω-ω_r . As the rotor is rotating with a relative speed of ω - ωr with respect to arbitrary dq reference frame.

The voltage equations of DFIG when modelled in 'dq' reference frame have inductances 'CsLssCs-1' and 'CsLsrCr-1' which are constant and also they are magnetically decoupled. Hence by 'dq' transformation all time varying and coupled inductances are transformed into constant and decoupled inductances. When the arbitrary reference frame is rotated with synchronous speed, i.e., when $\omega = \omega_s$ all the three phase quantities are converted into DC quantities and hence incase of control design all control problems are converted into final value problem which are easy to solve.

In 'abc' reference frame the all control problems are tracking problems which difficult to solve.

The electromagnetic torque produced by the DFIG is given by

$$T_e = \frac{3}{2}\frac{p}{2}L_m(i_{ds}i_{qr} - i_{qs}i_{dr}) \quad 3.44$$

$$T_e = \frac{3}{2}\frac{p}{2}\frac{L_m}{L_r}(i_{qs}\psi_{dr} - i_{ds}\psi_{qr}) \quad 3.45$$

Where p is no. of poles in DFIG; Finally,

The mechanical dynamics of the DFIG are described by

$$\frac{J}{p}\frac{d(\omega_r)}{dt} = T_e - T_m \quad 3.46$$

Where, *J* is the inertia constant; P is the no. poles; *Te* is the electromagnetic torque developed by DFIG and T_m is the shaft torque

3.4.3converter configuration

The back-to-back converter consists of two Voltage Source Inverters, i.e., Machine or Rotor Side Converter (MSC) and Parallel Grid-Side Converter (PGSC)**,** as shown in Fig. 2.7. Between the two converters a DC-link capacitor is placed, as energy storage, in order to keep the voltage variations (or ripple) in the DC-link voltage small. With the machine-side converter, it is possible to control the torque or the speed of the DFIG and also the power factor at the stator terminals, while the main objective for the grid-side converter is to keep the DC-link voltage constant.

Standard three phase bridge topology is employed for the converters. With a PWM converter in the rotor circuit, the rotor currents can be controlled in a desired phase, frequency and magnitude. This enables reversible flow of active power between the rotor and grid and the system can operate in sub synchronous and super synchronous speeds. The DC link capacitor acts as a source of reactive power and, it is possible to supply the magnetizing current, partially or fully, from the rotor side. The stator side power factor can thus be controlled. Using vector control techniques, the active and reactive powers can be controlled independently and hence fast dynamic performance can also be achieved.

Unlike the rotor side converter, grid side converter operates at the grid frequency. Flow of active and reactive powers are controlled by adjusting the phase and amplitude of the inverter terminal voltage with respect to the grid voltage. Active power can flow either to the grid or to the rotor circuit depending on the mode of operation. By controlling the flow of active power, the DC bus voltage is regulated within a small band. Since, the inverter operates at a high frequency, usually between; the harmonics in input current are greatly reduced.

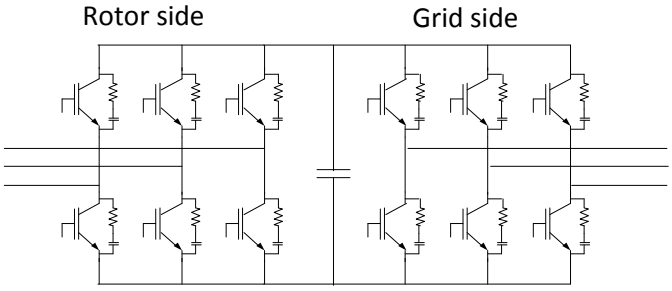

Fig. 3.7 Back-to-back connected power converter bridges.

It should be noted that, since the slip range is limited, the DC bus voltage is lesser in this case when compared to stator side control. A transformer is therefore necessary to match the voltage levels between the grid and the DC side of the PGSC. This arrangement presents enormous flexibility in terms of control of active and reactive powers in variable speed applications. In the following sections, model of the DC link is presented and also the control schemes of MSC and PGSC are discussed.

3.4. DC link model

The energy, E_{DC}, stored in the DC-link capacitor, C_{DC}, is given by

$$E_{DC} = \frac{1}{2} C_{DC} V_{DC}^{\ 2} \qquad 3.47$$

Where, V_{DC} is the DC link voltage.

Moreover, if the losses in the actual converter can be considered small and thereby be neglected. The rate of change of energy in the DC-link capacitor is dependent on the power delivered to the grid filter, *Pg* and the power delivered to the rotor circuit of the DFIG, *Pr*.

$$\frac{d(E_{DC})}{dt} = \frac{1}{2} C_{DC} \frac{d(V_{DC})^2}{dt} = -P_f - P_r \qquad 3.48$$

This means that the DC link voltage will vary as

$$C_{DC} V_{DC} \frac{d(V_{DC})}{dt} = -p_g - p_r \qquad 3.49$$

Which means that, if *Pf* = -*Pr*, DC link voltage will be constant.

3.5 Conclusions:

The model of the system has been successfully developed, which has given a good insight of the subject and intricacies involved. The sizing of the components etc has been done based on the analysis and model so developed. More over the clarity of the control scheme to be adapted become clearer.

CHAPTER4
Control of DFIG

4.1 General

A typical farm of WECS with its different components may be depicted in Fig. 4.1. For instance a system of 9 MW wind farm may be equipped with 6 x 1.5 MW variable-speed DFIG wind turbines and grid supply connection. The wind turbines are generally considered operating under identical operating conditions for modelling purpose individual WECS unit is controlled to operate in a way such that each unit remain synchronised with the grid.

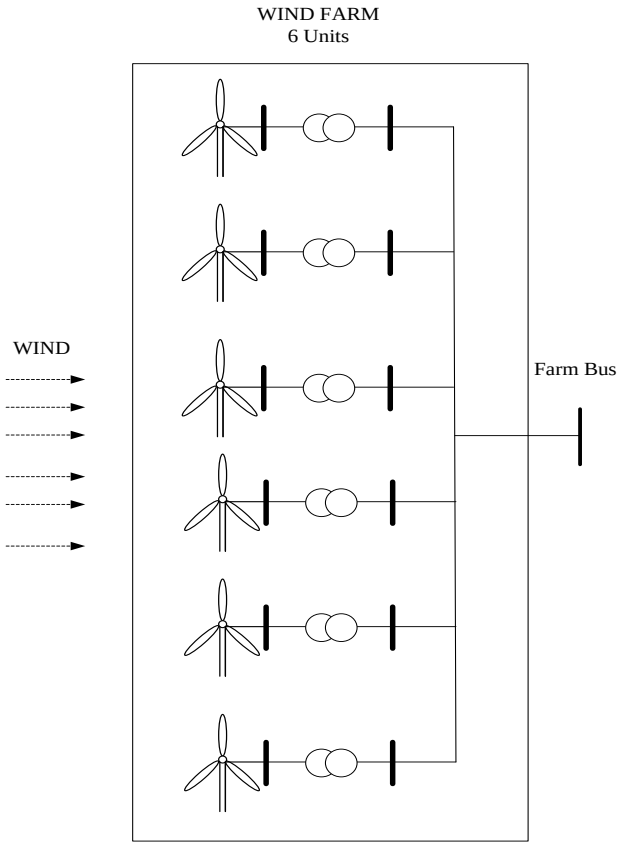

Fig.4.1 Grid connected wind farm system

In this chapter new control scheme for DFIG for its rotor and grid side converter controller structures has been presented. As control design is a major

concern, model of system developed in previous chapter is utilised to access the limitations and control options are available WECS.A detailed control structure and model of WECS using DFIG is presented. The system is controlled by new proposed current controlled scheme for operation insensitive to connected load and parametric variations. The proposed closed loop control offer faster and easier control which could be easily implemented.

4.2 Control Techniques for DFIG

The typical DFIG configuration, illustrated in Fig. 4.2 consists of a wound rotor induction generator (WRIG) with the stator windings directly connected to the three-phase grid and with the rotor windings connected to back-to-back power converters in the rotor circuit. The back-to-back converters are bi-directional voltage source converters namely rotor side and grid side converter – see Fig4.1) and share a common dc-bus. The power flow in WCES is also shown in Fig.4.2 The stator side power transfer takes place at fundamental frequency whereas the rotor circuit side operate at slip frequency. When speed falls in super synchronous mode power flows out of the rotor circuit and when the speed is within the sub synchronous range the power is fed into the rotor circuit.

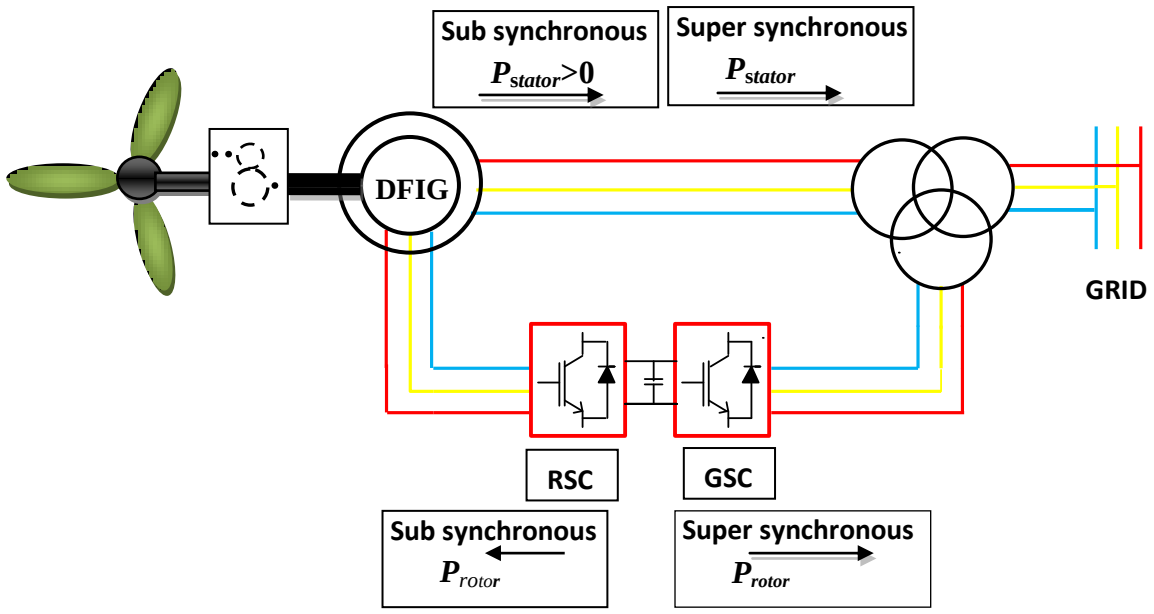

Fig.4.2 Block diagram of DFIG

4.2.1 Voltage and frequency control methodology

The stator of DFIG is directly connected to the three-phase grid, while the rotor winding is connected to grid via two bi-directional power converters, the RSC operating at slip frequency and GSC operating at fundamental frequency. For the variable speed operation the converters operate in such a way that power is extracted from rotor for super synchronous speeds and vice-versa for sub synchronous speeds. This makes the converters to operate in four-quadrants. For integration of large wind farms into utility grid, the terminal voltage of DFIG must be same as of the up coming grid, and frequency synchronized with the marks. A control strategy based on the stator voltage and frequency as control variables, and using vector control technique, both voltage and frequency may be controlled independently by controlling the rotor d-axis and q-axis currents which is so called indirect current control. The details of the control scheme developed with current control are presented in the fourth coming section 4.4 of this chapter.

4.2.2 Decoupled power control

The vector control techniques allow de-coupled control of active and reactive power. The current and the voltage are transformed in the rotating reference frame to yield the active and reactive powers, when the reference frame is synchronised with phase voltage the d-axis rotor current represents the active component of the current may be used to regulate real power transaction. Whereas, the q-axis current represent the reactive component of the current and they may be used to regulate reactive power. The current control technique offer faster response. Through hysteresis current control a new method using indirect current control of the d-q axis current templates may be employed for the control of RSC to control the transaction of real and reactive power by the DFIG.

4.3 Hysteresis current controller

The current control methods play an important role in power electronic circuits, particularly in current regulated PWM inverters which are widely applied in ac motor drives and continuous ac power supplies where the objective is to produce a sinusoidal ac output. The main task of the control systems in current regulated inverters is to force the current vector in the three phase system according to a reference trajectory [40]. Among the various PWM techniques, the hysteresis band current control is used very often because of its simplicity of implementation. Also, besides fast response current loop, the method does not need any knowledge of load parameters. However the current control with a fixed hysteresis band has the disadvantage that the PWM frequency varies largely.

Pulse width modulation methods involve the synchronization of the reference waves with the desired output waveforms, and a high degree of precision in generating wave forms. While feeding power into the utility network through the DC link inverter, the output current and its phase become the control variables with regard to power transfer at constant grid voltage. Hence, it is desirable for the PWM control to be associated with the system current control. Two current controllers for voltage fed PWM inverters namely the hysteresis controller and the ramp comparison controller are in wide use.

One does not require any information about the system parameters in order to use these controllers. In both the methods, three phase reference sine waves proportional to the desired currents, based on certain criteria are generated and compared with the measured instantaneous values of the output currents. To keep the deviation within the prescribed limits, the comparator error is then processed through a controller generating signals to turn on or turn off the appropriate switching devices of a conventional PWM VSI as shown in Fig.4.3 (a).

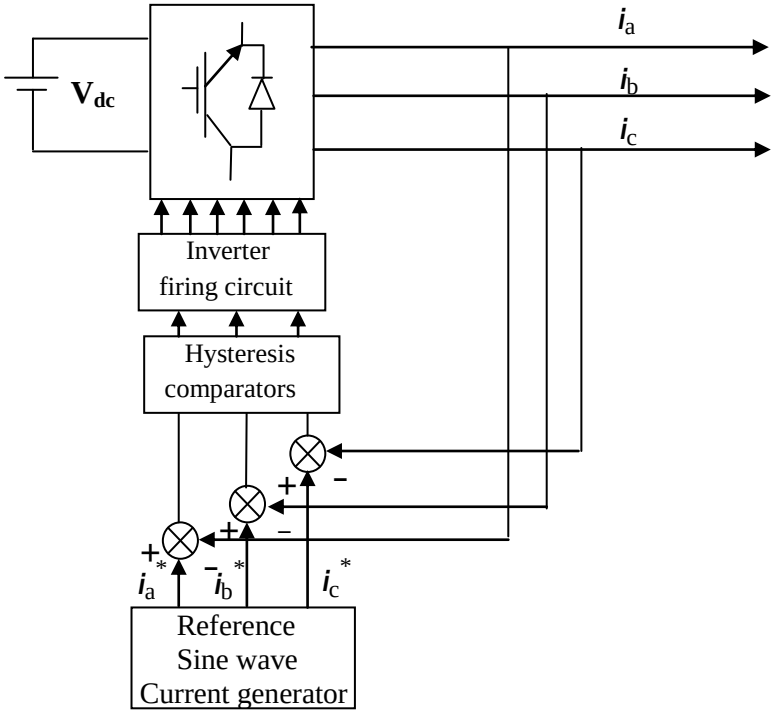

Fig.4.3 (a) Block diagram of the three phase PWM inverter with hysteresis band current controller.

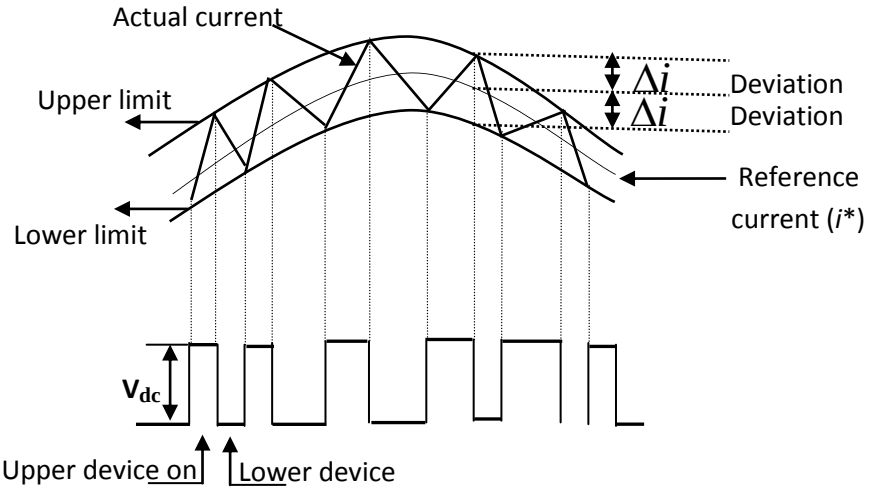

Fig.4.3 (b) Inverter output current and voltage wave forms with sinusoidal reference current

Above fig4.3 (a) shows the block diagram of the basic control and power circuit. Fig4.3 (b) shows illustrates the principle of the hysteresis band current control.

The hysteresis comparator has a dead band that permits a deviation of Δi of the actual current from the reference wave. If an actual phase current exceeds the current

reference by the hysteresis band, the upper device in the inverter leg of that phase is turned off and the lower device is turned on. This causes the phase current to decay until the current error reaches the lower limit when the switch status is reversed, causing the current to rise again. Independent control of phase current is possible in this manner if the three phase load neutral is connected to the DC bus midpoint. In a system without such a neutral connection, the current response of a phase depends not only on the switching state of the corresponding leg but also on the status of the other two inverter legs. For loads with unconnected neutrals, the instantaneous current error can take double the hysteresis band.

4.4 Control Strategy for Converters

The vector control techniques allow de-coupled control of active and reactive power. These techniques are based on the concept of d-q transformation reference frames, where the current and the voltage are transformed into distinct components in synchronised reference frame related to the active d- axis, reactive q- axis components.

4.4.1 Voltage and frequency control

The voltage generated by DFIG and its frequency are controlled independently by controlling the currents injected in the rotor of DFIG. Change in frequency occurs when an active power transaction occurs by load variations and change in magnitude of the voltage occurs when reactive power transacted by stator circuit. The proposed control technique for the rotor side converter uses direct axis current component for control of frequency and quadrature axis component for the voltage control. A very fast closed loop control regulates the active and the reactive component of the rotor current to effect the desired compensation of frequency and magnitude of the voltage at the stator terminals. Whereas, the **GSC** regulates the flow of active power transaction by rotor circuit through regulation of DC bus. The fallowing section deal with details of the control scheme adopted for **GSC** and **RSC**. For the proposed Control scheme.

4.4.1.1 Grid side converter control

The aim of grid side converter is to maintain the dc bus voltage at constant value irrespective of direction of power flow, A reference dc voltage is compared with the capacitor averaged instantaneous dc voltage and the error value fed to a **PI** controller which generates the reference current i_d, the generated component i_q is taken as zero and then i_{dq} current is transformed into i_{abc}^* which acts as reference currents for grid side converter. A hysteresis current controller operates on indirect current control to make the current i_{abc} close to i_{abc}^*. The scheme is shown in Fig4.4. The PLL used for transformation to dq reference frame operates in line frequency. The closed loop control scheme is depicted in fig 4.5.

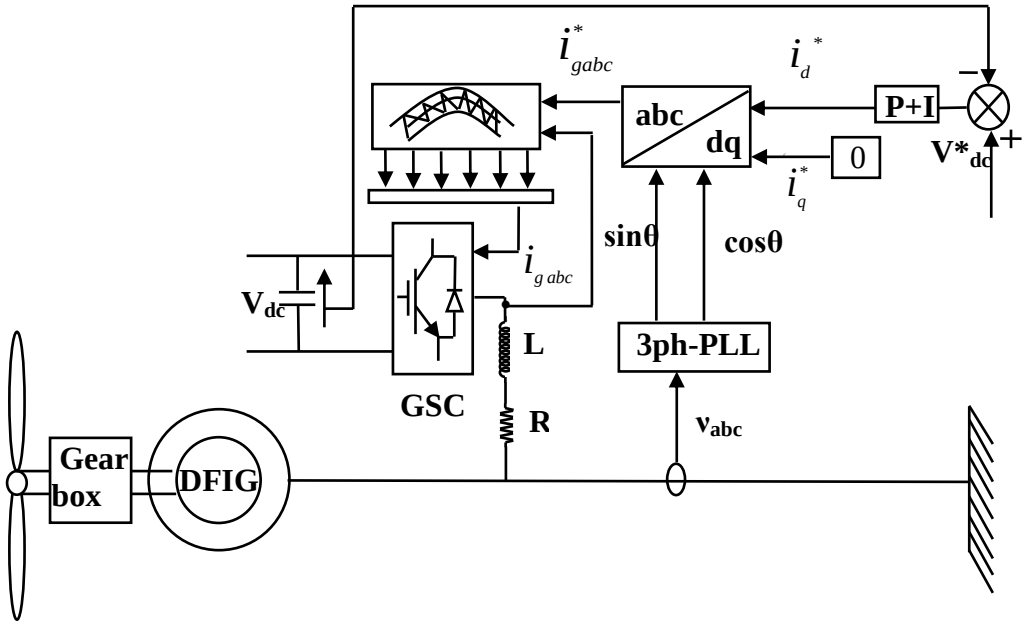

Fig.4.4 Schematic diagram of control scheme for **GSC**

4.4.1.2 Rotor side converter control

The aim of the rotor side converter is to control independently the stator voltage and frequency. The voltage and frequency are not controlled directly, but by controlling the real and reactive components of the rotor current at slip frequency. A fixed frequency is compared with the instantaneous **PLL** based measured frequency of the stator side voltages. The error fed to the **PI** controller which in turn gives a reference d-axis rotor current responsible for maintaining frequency. A synchronously reference voltage corresponding to the grid voltage is compared with the instantaneous measured voltage by transforming the three phase quantities in dq frame and finding out the **rms** value in the dq frame. The error fed to the **PI** controller which computes the q-axis reference rotor current responsible for maintaining the voltage at stator terminals, the d-q rotor currents so obtained are transformed into abc frame and fed to hysteresis controller along with the instantaneous sensed rotor currents which in turn generates switching patterns for the **RSC** converter.

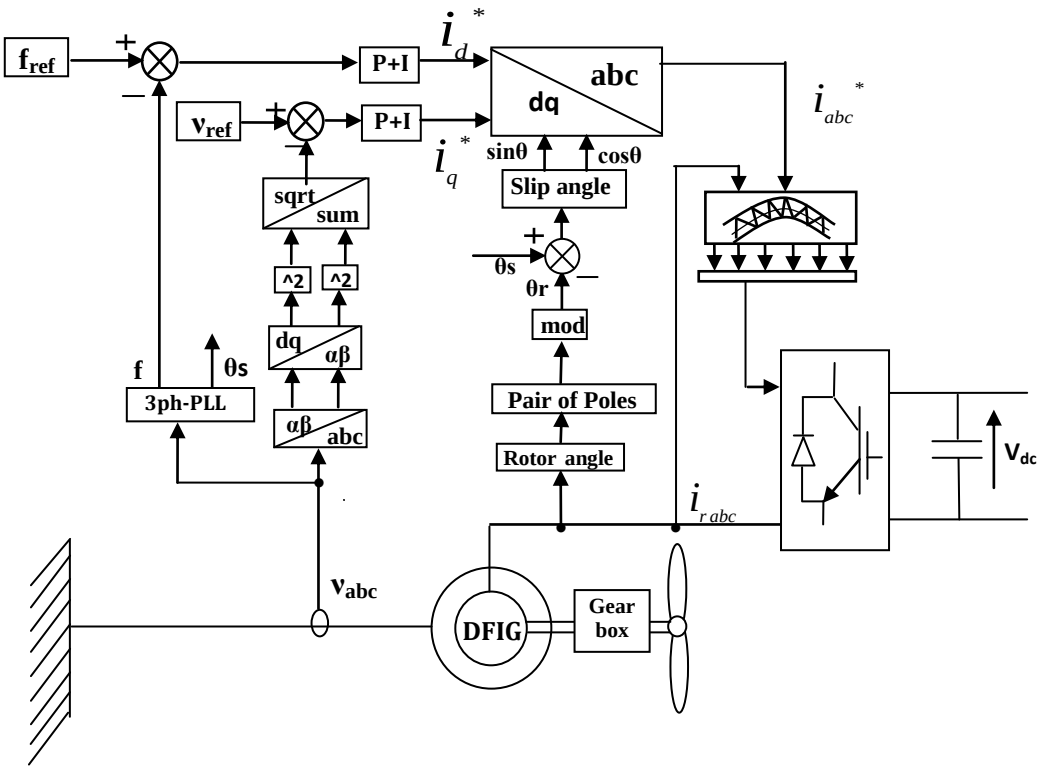

Fig.4.5Schematic diagram of control scheme for rotor side converter

4.4.2 Decoupled power control

The decoupled power based control scheme is illustrated in Fig 4.6 the electrical control of the **RSC** employs vector control technique. The grid side converter control computes the d-axis current reference with the help of a PI controller which operates on error between the measured value of the capacitor voltage and the reference dc bus voltage (V_{dc}). The q-axis current is taken to be of zero value reflecting the case when no reactive power transacted by **GSC.** The currents so computed are transformed into abc components, and subsequently fed to a hysteresis current controller which operates on the error computed between the instantaneous measured currents at the grid side converter and the reference current so computed by the control scheme. The switching pulses generated by the hysteresis current controller operate the GSC for regulating the dc bus voltage at constant level.

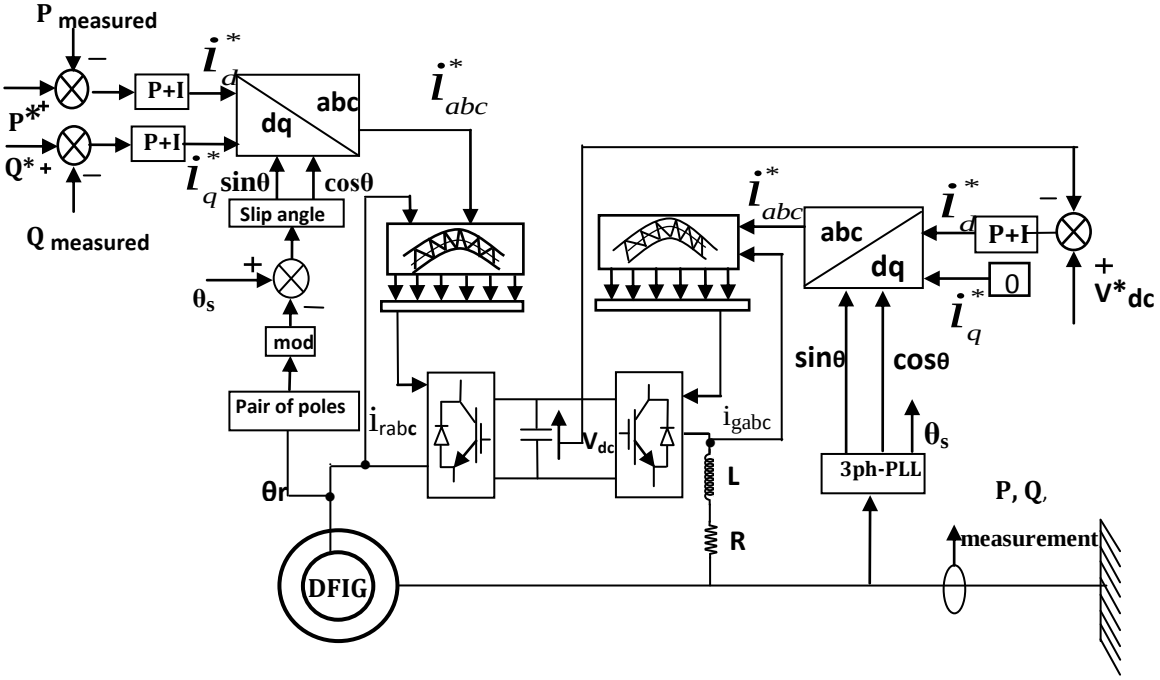

Fig.4.6 Schematic diagram of control scheme for the decoupled power control.

On the other hand the rotor side converter operates on the methodology of control active and reactive power independently, .the error generated by comparison of measured active power with the reference active power is fed to the **PI** controller, and the **PI** controller in turn computes the reference d-axis rotor current. In similar way measured reactive power, and the error is given to the **PI** controller which in turn computes the reference q-axis component of rotor current. These d-q components of reference rotor currents are transformed into abc components. The reference currents are compared with the instantaneously measured rotor currents, and the error so generated is fed to hysteresis current controller. The hysteresis current controller provides switching patterns for the gate of the power electronic switches of the **RSC.**

4.5 MATLAB Model of DFIG

The WECS is modelled in MATLAB Simulink using Simpower power system block set. The model of asynchronous machine is readily available in the block set which is utilised in simulation purpose. A model of wind turbine is simulated as per the Eqs [1.1-1.3] given in chapter1, the block of wind turbine is also developed in Fig4.7 the subsequent sections deals with the MATLAB model of the proposed new control scheme of the DFIG.

4.5.1 Voltage and frequency control

Fig. 47 shows the complete MATLAB model of WECS with the DFIG, two bidirectional power handling converters namely GSC and RSC, Subsystem having control mechanism subsystem, dc bus capacitor, and a data acquisition subsystem. The subsystem control having the control strategies to control both the grid side converter and rotor side converters independently by giving appropriate switching pulses to the gate terminals of the converters. The function of data acquisition system is to calculate the power developed by the machine. A wind turbine which develops the torque as per the equations studied in chapter1.

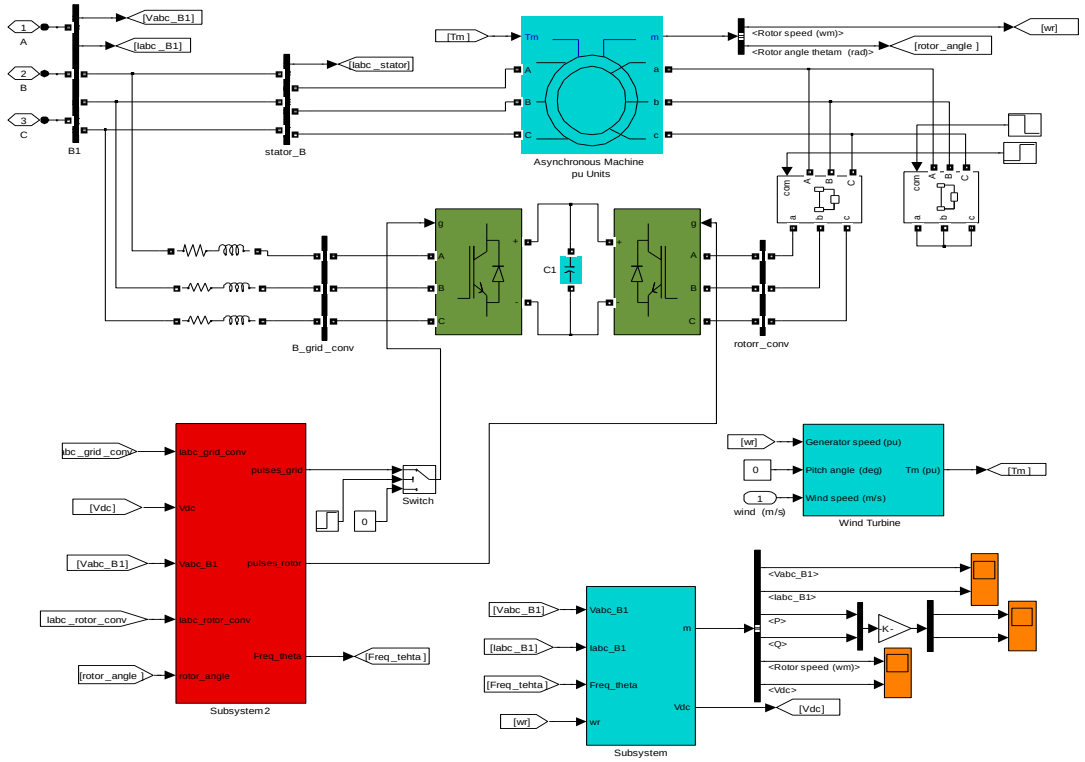

Fig.4.7 MATLAB block diagram of the DFIG with the complete control technique

4.5.1.1 Grid side converter

Fig.4.8 Shows the MATLAB model of the grid side converter (GSC) control scheme for voltage and frequency control which is having a reference i_d current generator block, a Simpower system block let for trans forming dq0 components to abc components, and a hysteresis current controller which generates switching pulses for the grid side converter to regulate the DC bus voltage at a constant value.

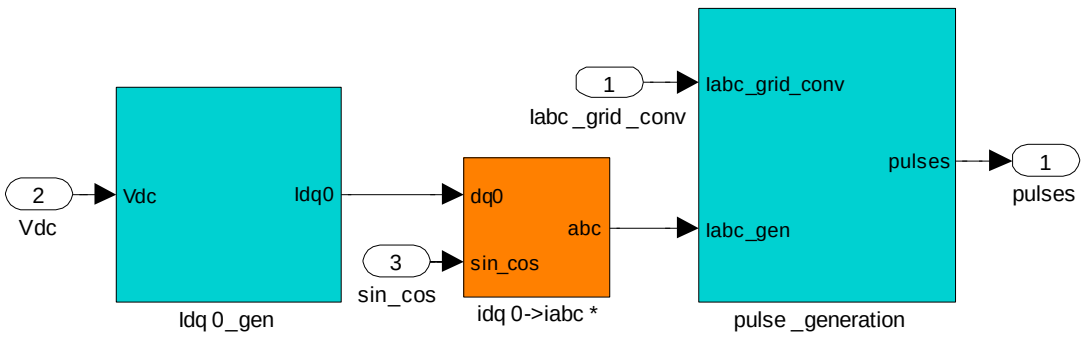

4.8 MATLAB block diagram of control scheme for grid side converter control

4.5.1.2 Rotor side converter

Fig.4.9 shows the MATLAB model of the rotor side converter to control the stator voltage and frequency, in this model a subsystem calculates the stator frequency, and v_d, v_q components of stator voltages, and two sub systems to calculate reference i_d, i_q currents, A transformation block to transform dq0 to abc, and a hysteresis current controller to generate switching pulses for RSC.

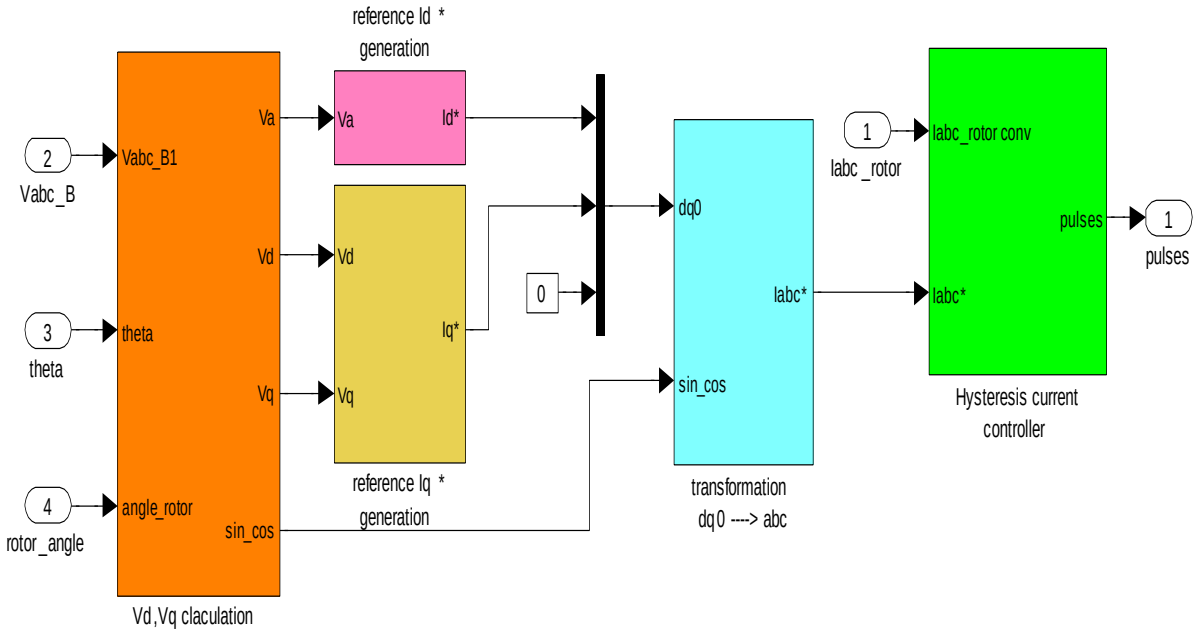

4.9 MATLAB block diagram of Control scheme for Rotor side converter control

4.5.2 Decoupled power control

Fig. 4.10 shows the complete MATLAB model of complete wind energy system with the DFIG, which containing two converters is called GSC and RSC, wind turbine, control system block, the control system is a sub system which is having control mechanism to control DFIG by giving proper switching pulses to the power converters.

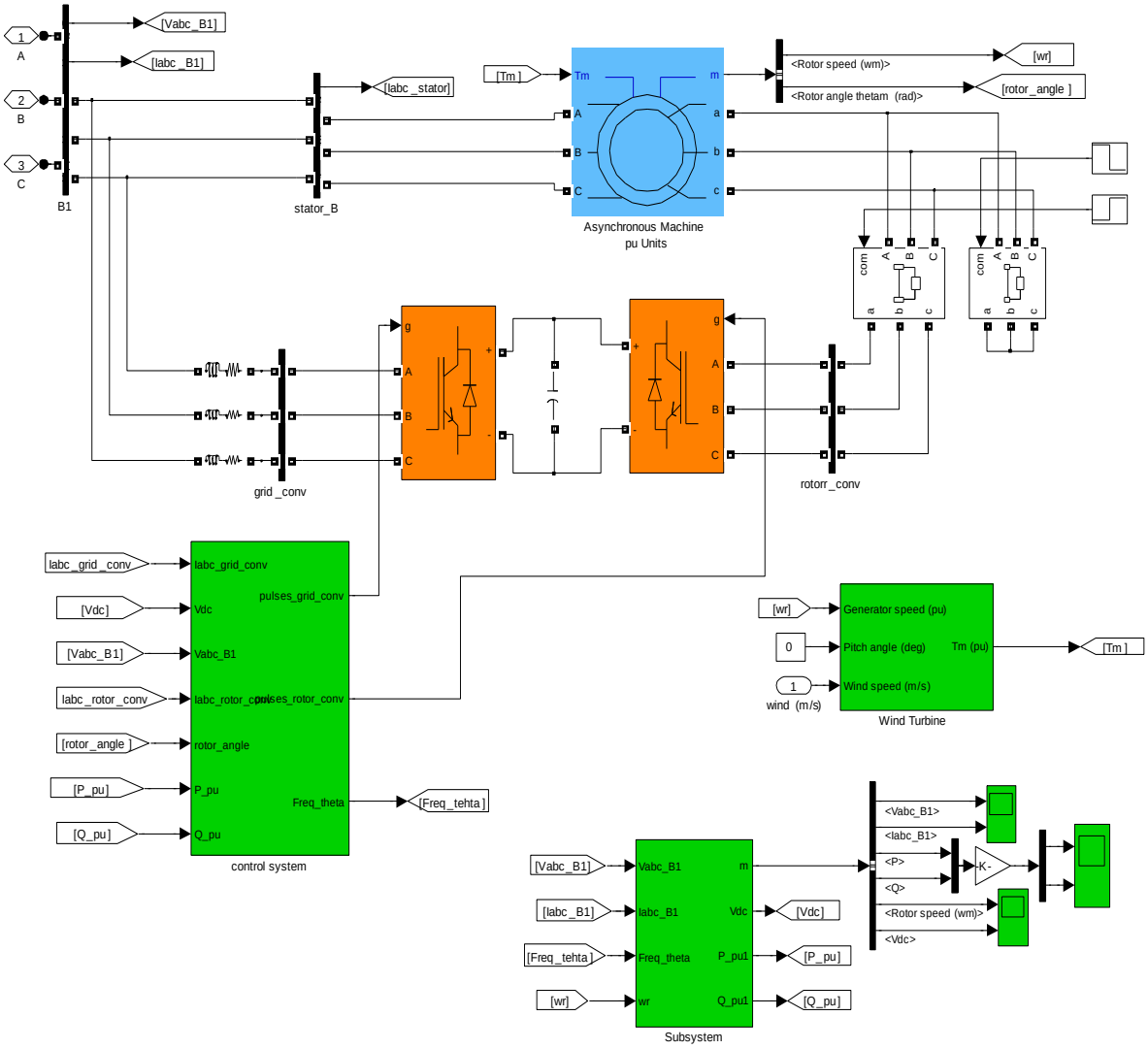

Fig.4.10 MATLAB/Simulink block diagram of the DFIG with the complete control technique

4.5.2.1 Grid side converter

Fig.4.11 shows the MATLAB model of the grid side converter to control the dc bus voltage, it consists a reference id current generator, a transformation block to transform i_{dq0} to i_{abc}. And a hysteresis current controller to control the GSC by developing appropriate switching pulses.

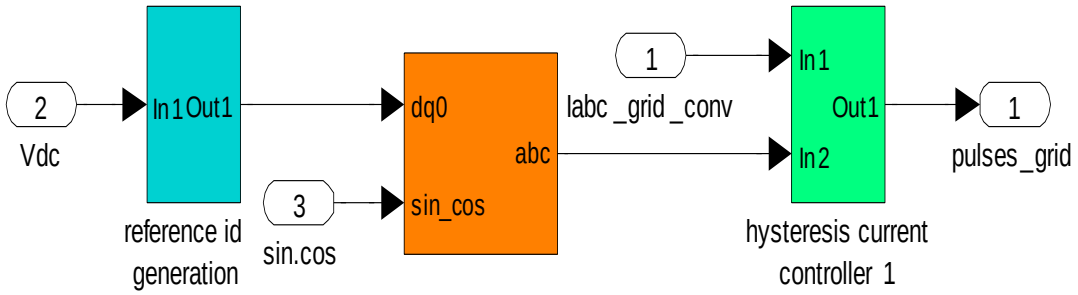

Fig4.11 MATLAB block diagram of control scheme for grid side converter control

4.5.2.2 Rotor side converter

Fig.4.12 Shows the MATLAB model of the rotor side converter control scheme for decoupled power control. In this block it is having a slip angle calculation block, power controller which generates reference i_d, i_q currents, and a hysteresis current controller.

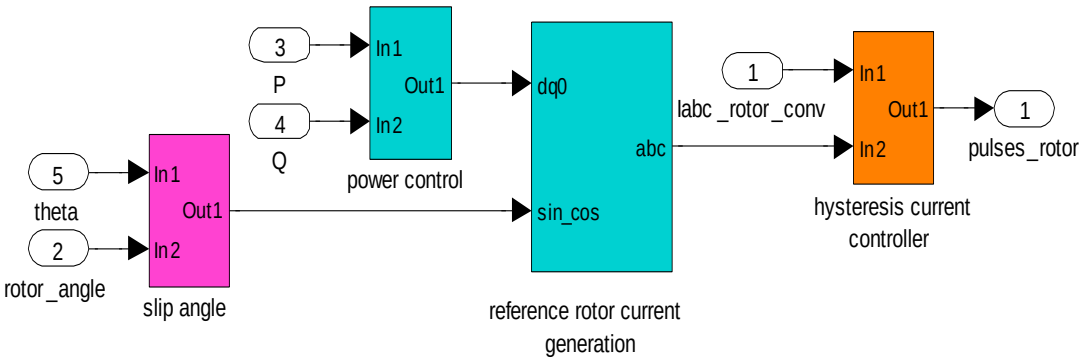

Fig.4.12 MATLAB block diagram of Control scheme for Rotor side converter control

4.6 Results and discussion

The wind energy conversion system i.e., wind turbine and doubly fed Induction generator along with proposed control loops for grid-side converter and rotor side converter are modelled in MATLAB/Simulink. The ratings of the DFIG (doubly-fed induction generator), wind turbine and the simulation parameters of the system are presented in the Appendix. The performance of the system has been depicted in Figs.4.13-4.20.

Figs.4.13-4.14 shows performance of the voltage and frequency controller for the DFIG for a fixed wind speed of 10 m/s. Transient/steady state waveforms of the generator voltage V_{abc}, frequency of generated voltage, dc-bus voltage V_{dc}, active power P(MW),reactive power Q(MVAR),rotor speed ω_r ,wind speed V_w(m/s) are shown. We consider the system started as cage rotor machine at t=0 and then switched to wound rotor at t=1 and proposed control scheme is applied at the same instant. At this instant a voltage dip occurs at dc bus and stator terminal voltage. The machine out put voltage is settled within 0.1 sec as the controller settles the switching transients. The dc bus voltage dip takes about 1 sec to settle after the controller action. The active power before the control action was close to 9MW and fluctuating as can we seen in Fig. After the controller action the active power settles at about 5MW and Fluctuations are settling down. The reactive power drawn by the machine before the control action was huge which after application of controller action settles down to 2.8MVAR. The rotor speed which was 1.09 at the starting of the machine after the control action, has now settled at 1.042pu.

Fig [4.15] shows the results of DFIG under a condition of grid voltage sag. as can be seen from the figure at time t =4sec a sudden change of grid voltage from 1.0 to 0.8 causes an unbalance in the network, the frequency oscillations are settled in 0.2 sec ,the rotor current is within the limit and settles down in 0.2sec,dc bus voltage dip takes about 1sec to attain a reference voltage, there is no appreciable change in rotor speed because of grid voltage dip, with the dip in grid voltage the active power decreases and at this instant DFIG tries to maintain the terminal voltage by reducing the reactive power requirement. Voltage by feeding reactive power to the grid. in fig [4.16] shows the simulations with symmetrical voltage sags We can see that the rotor current can be limited within the maximum rotor current of converter, and the dc-link voltage changes is small, which show that the controller proposed in this can

successfully reduce disturbances from symmetrical voltage sags such that nominal power production can be restored once the grid voltage recovers.

The performance of the decoupled active and reactive power controller for the dfig is demonstrated with a fixed wind speed of 10 m/s and a variable wind speed of 10m/s mean value with a turbulence of 5% and 1m/s up and down, simulated transient/steady state waveforms of the generator voltage V_{abc}, dc-bus voltage V_{dc}, active power P(MW),reactive power Q(MVAR),rotor speed ω_r ,win speed V_w(m/s) are shown in fig [4.17],[4.20] .

Fig [4.17] shows the simulated starting transient wave forms of the dfig, at time t=2sec the proposed control scheme is applied, and results were observed, the stator generated voltage Vabc is at 1 pu, dc-bus voltage is maintained at 1200(volts), the power delivered to the grid (stator power +slip power) is 5 (MW), the machine is operating under super synchronous speed. Fig [4.18] shows the simulated results of DFIG depicting blow up of condition with decoupled power control

Fig [4.19] shows the results of DFIG at variable wind speed the wind speed is supposed to have a mean value of 10m/s with a turbulence of 5% and 1m/s up and down variations. The figure shows that the stator output voltage is constantly maintained at 1pu and dc bus voltage is also maintained at 1200(volts).the active and reactive power are changing with the rotor speed which is maintained by the controller. Fig [4.20] shows the steady state waveforms of the dfig.

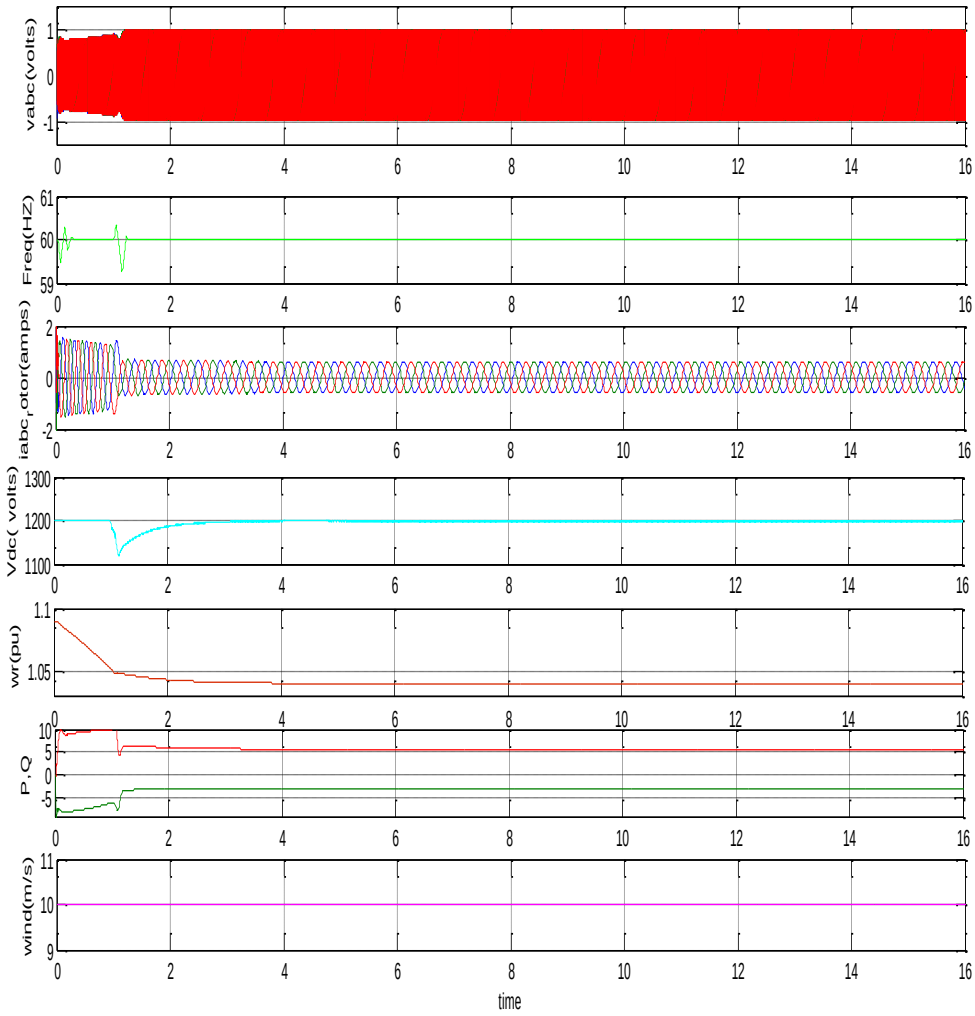

Fig.4.13 Simulated results for starting transients of DFIG with 10m/s wind speed using voltage and frequency controller.

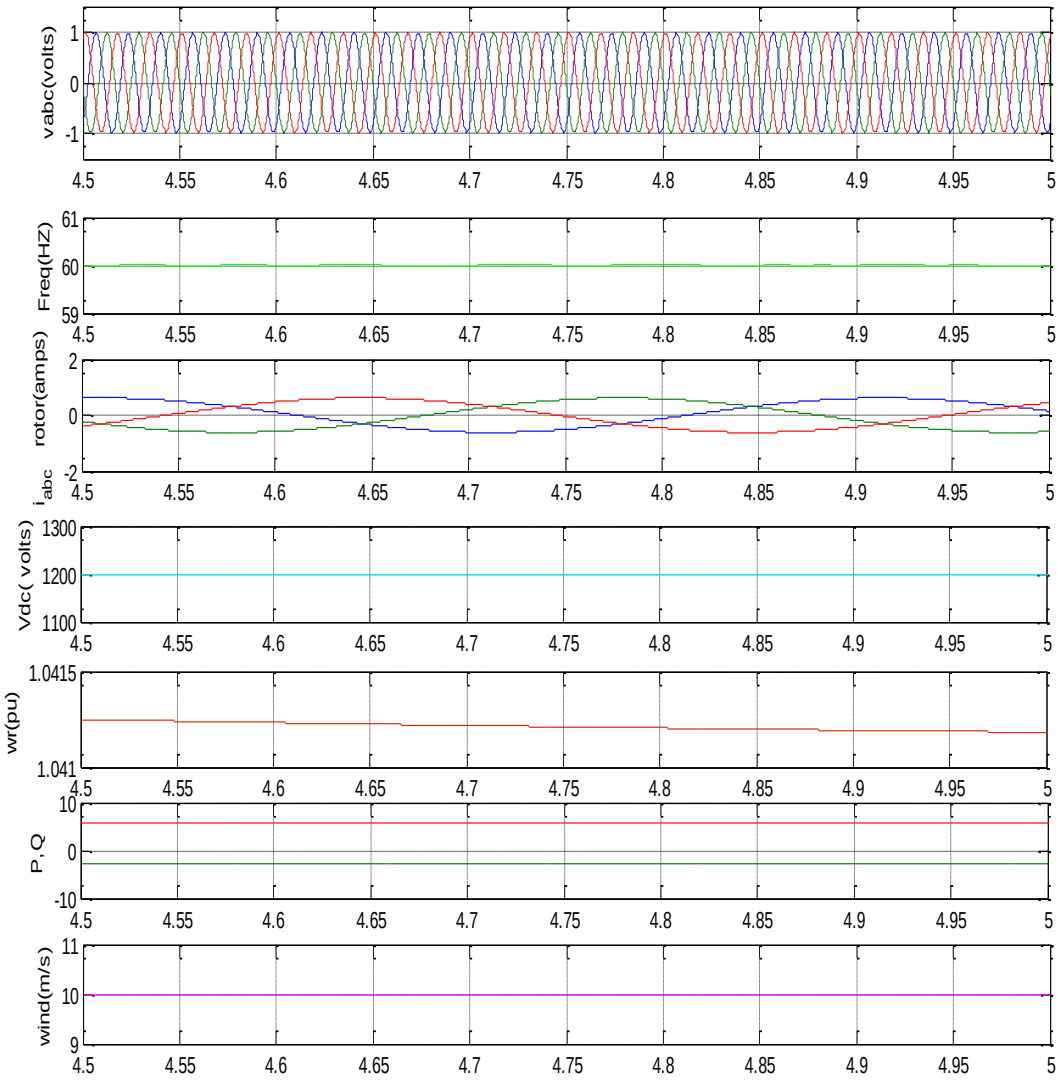

Fig 4,14 Simulated

Fig.4.14 Simulated results under steady state conditions of DFIG with 10m/s wind speed by using voltage and frequency control method.

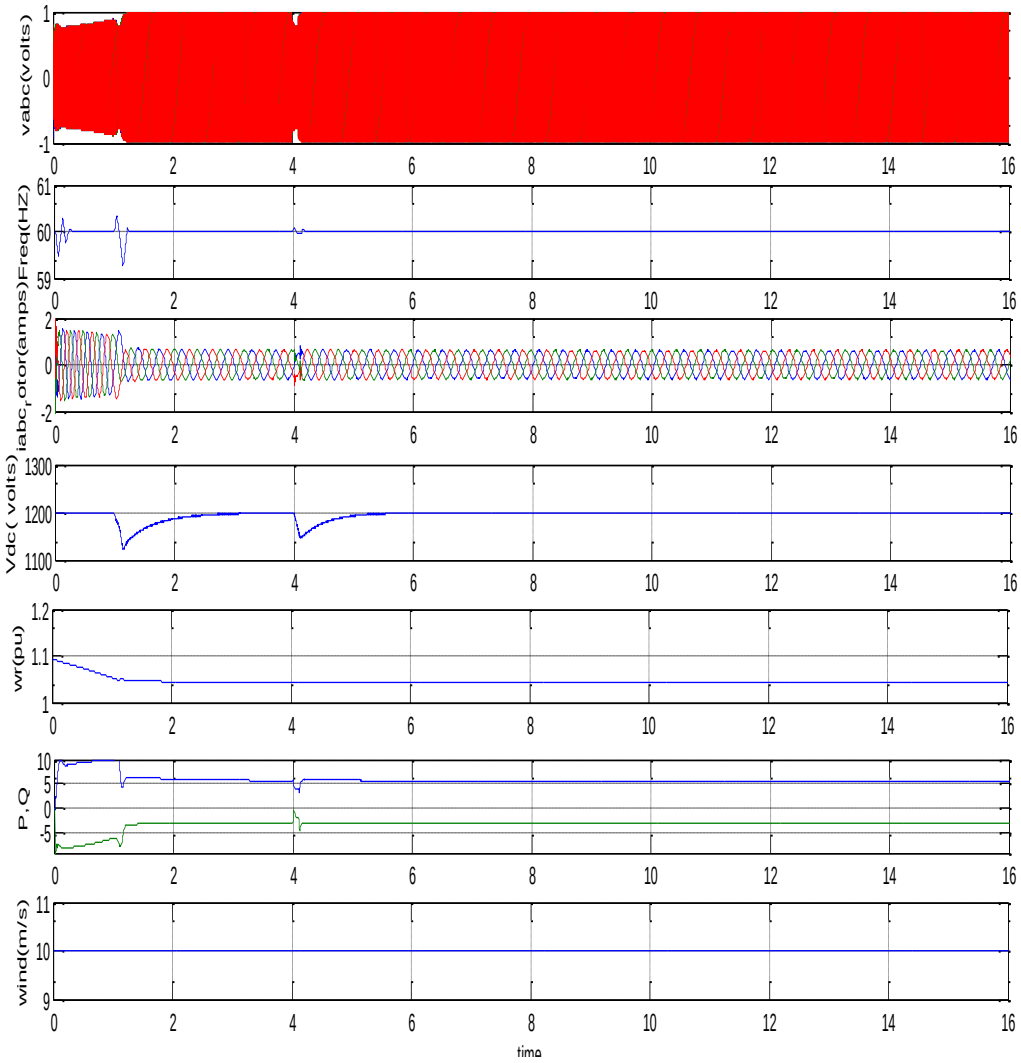

Fig.4.15Simulated starting transient of DFIG with under grid voltage sags by using voltage and frequency control scheme

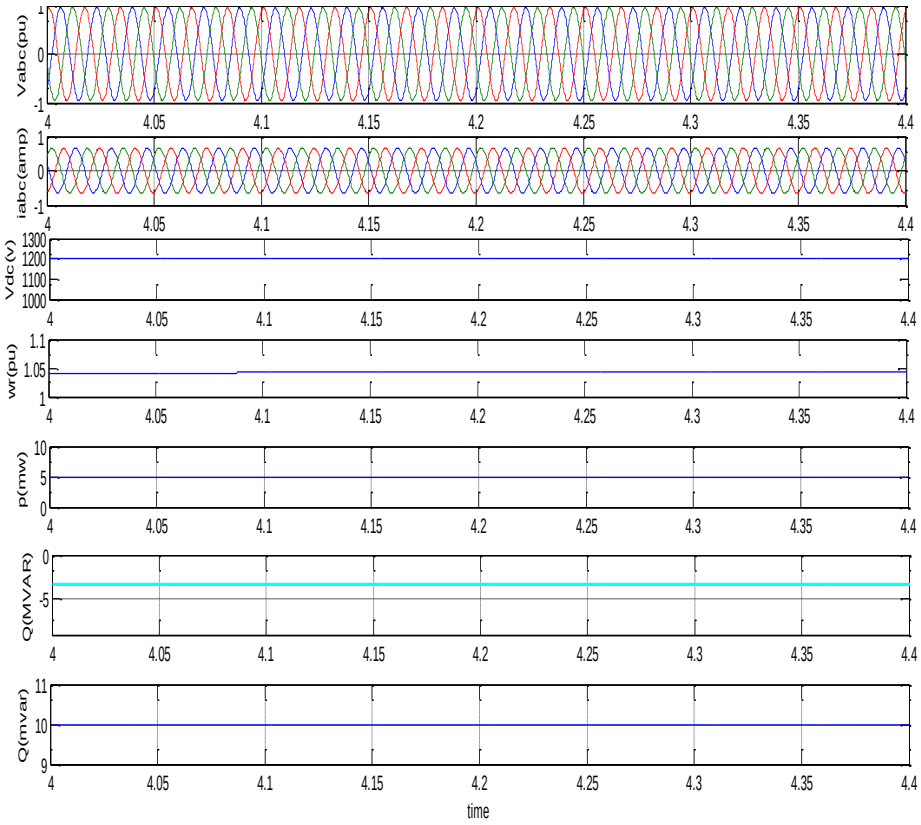

Fig.4.16Simulated results of DFIG depicting blow up of condition under grid voltage sags.

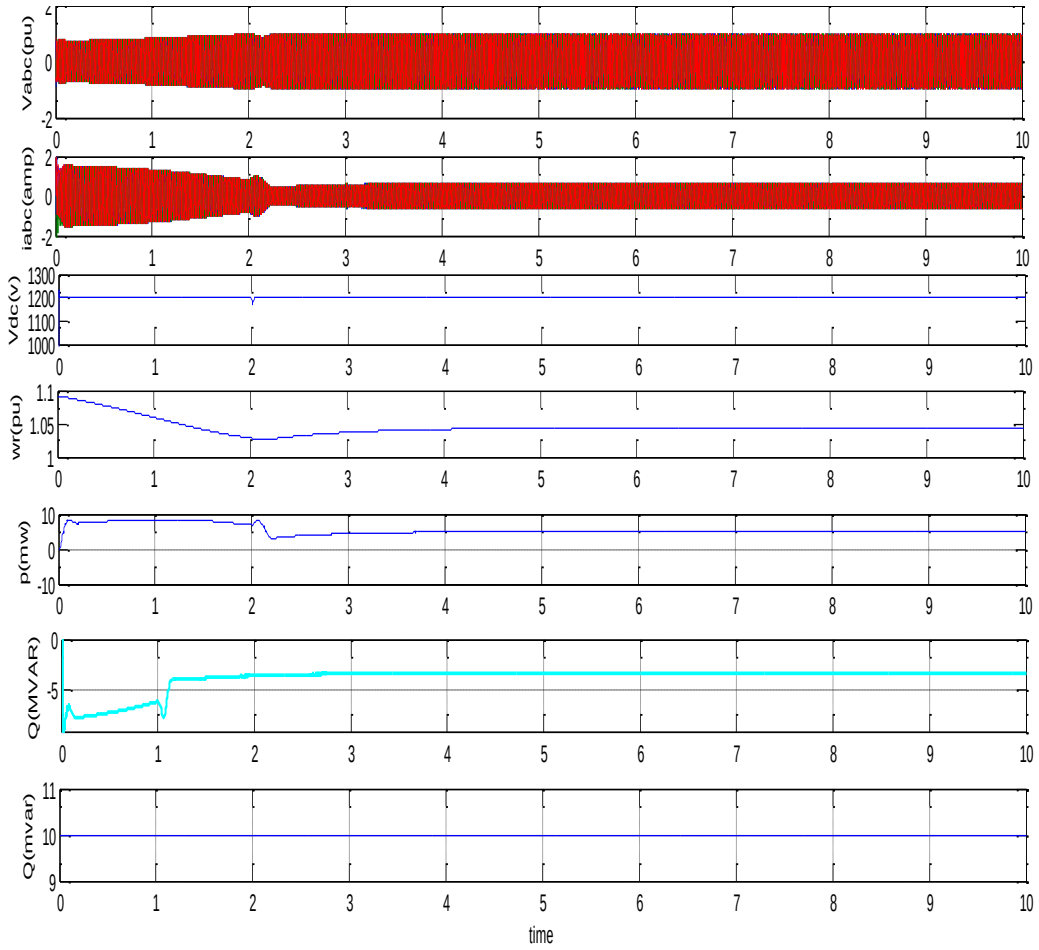

Fig.4.17 Simulated starting transient results of DFIG with 10m/s wind speed with decoupled power control scheme

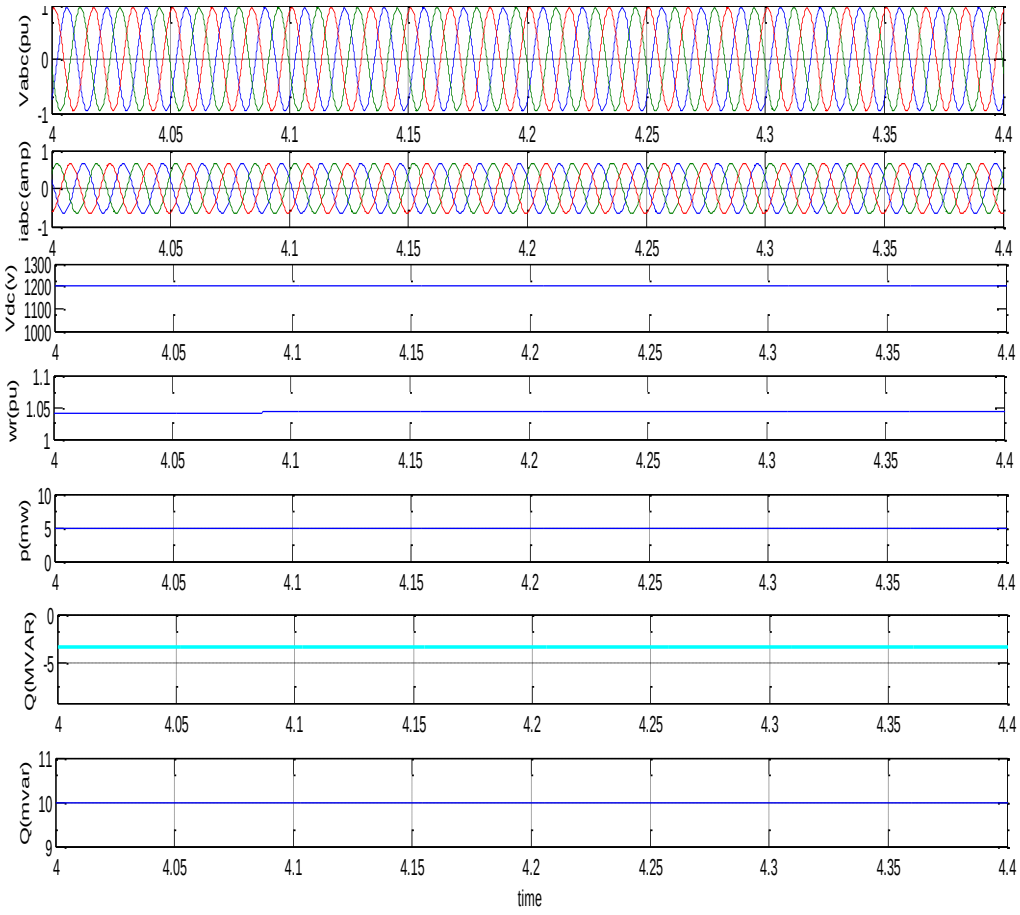

Fig.4.18Simulated steady state results of DFIG with 10m/s wind speed with decoupled power control scheme

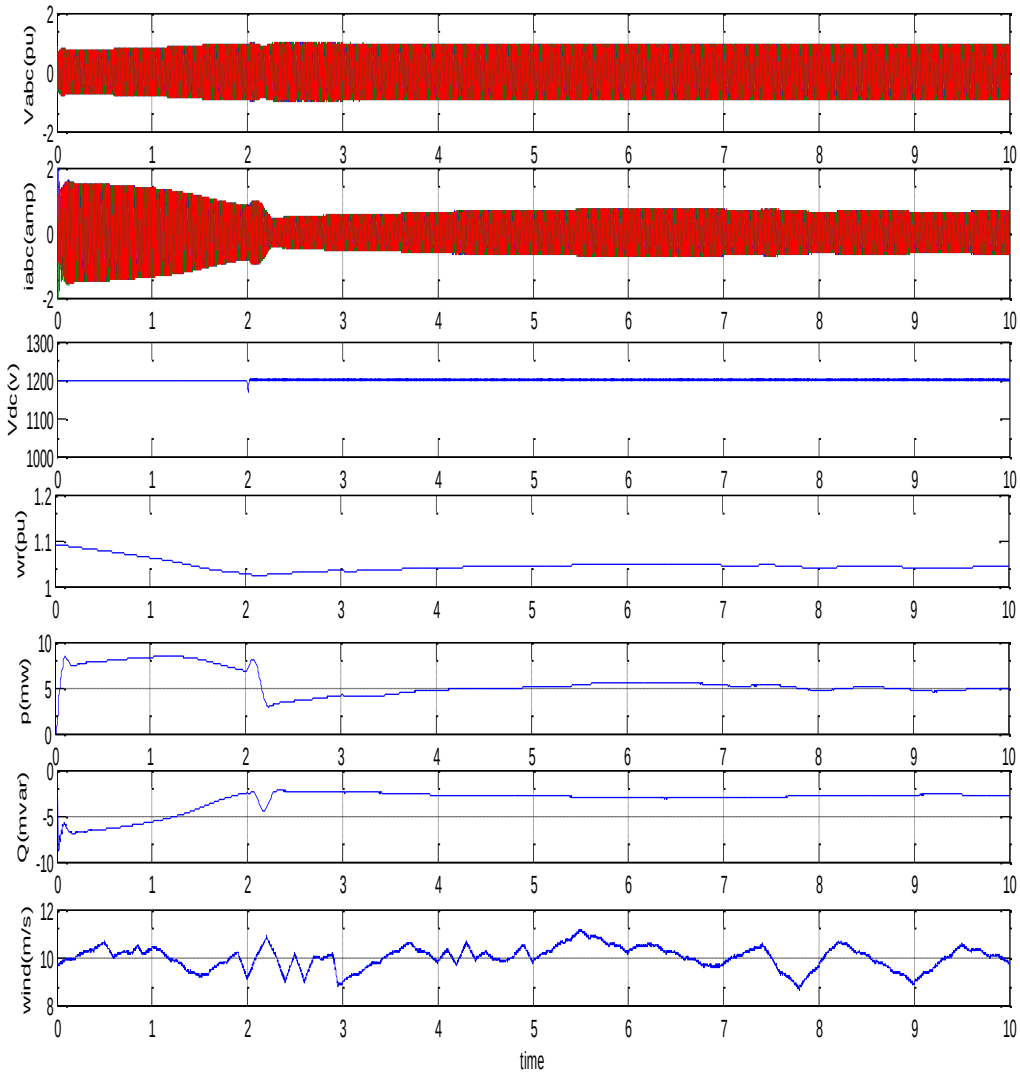

Fig.4.19 simulated transient results of DFIG with 10m/s mean value with a 5% turbulence and 1m/s up and down

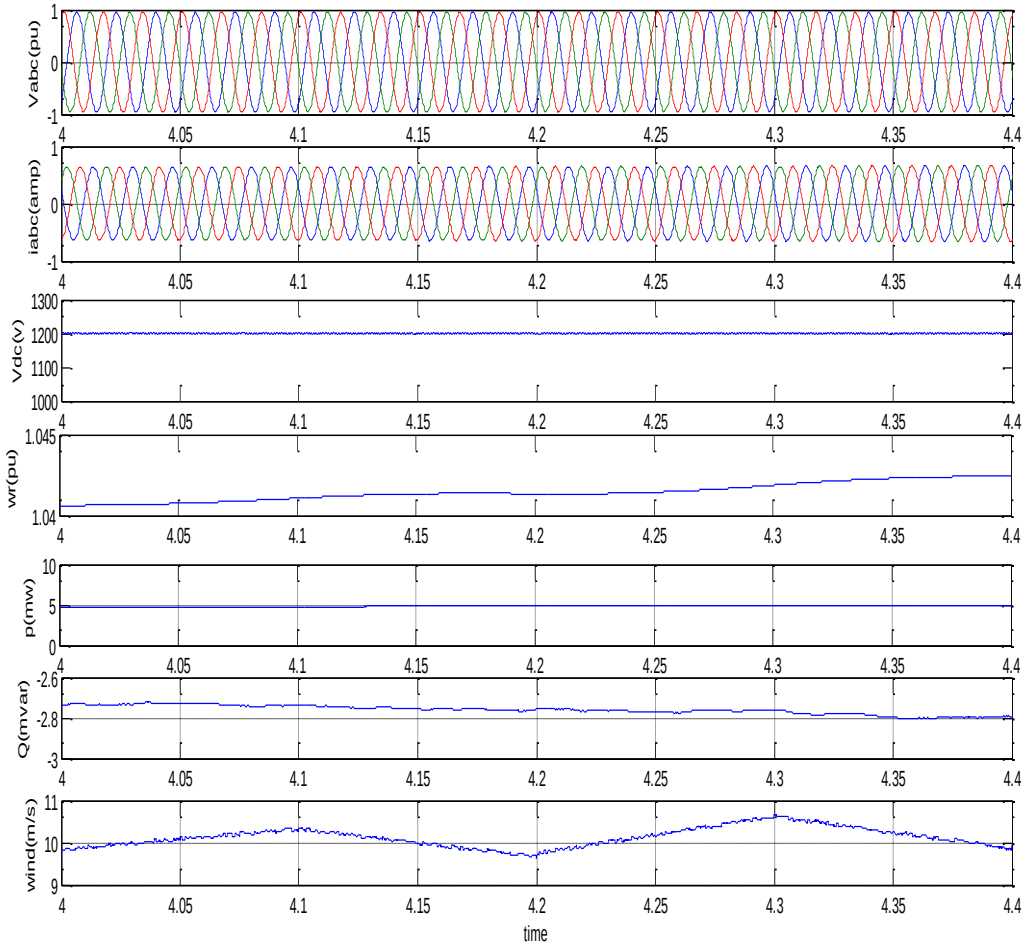

Fig.4.20 Simulated steady state results of DFIG with 10m/s mean value with a 5% turbulence and 1m/s up and down

4.7 Conclusion

The performance of DFIG with different dynamic conditions are studied with both types of control schemes,

One control scheme operates through indirect current control on regulation of frequency and terminal voltage of the DFIG insensitive to any parametric variations of machine and load dynamics. In addition to this the control offers flexibility in power exchange through rotor circuit at unity power factor with very low THD.

The second control scheme operates on decoupling of active and reactive power. The current control forces the DFIG to follow the reference power inputs and in a way can extract maximum power from the wind turbine.

Chapter 5

Conclusions and suggestions for further work

5.1 General

The main objective of the work has been to model the Wind Energy Conversion System employing DFIG (doubly-fed induction generator). The model consists of wind energy turbine, Grid connected DFIG, its new control schemes. The WECS with two new control schemes has been simulated under various conditions and results have been presented in previous chapters.

5.2 Main Conclusions

The WECS equipped with DFIG along with two voltage source converters (VSCs) in the rotor circuit has been investigated. The main focus of the study has been towards the development of the control schemes that are simplified and easy to implement, offer faster dynamics, have flexibility, robust in operation and are insensitive to parametric variations of machine and load variations in the grid. Besides these efforts have been made to provide features in the control to support the DFIG to coexist in the wind farm and also support other DFIG short of reactive power. The control techniques so developed operate on the stator voltage and frequency with indirect current control. The main conclusions are:-

- A model of wind turbine which imitates the actual wind conditions has been developed and modeled under MATLAB/SIMULINK.
- Model of DFIG using asynchronous machine model from power system block set has been developed.
- Model of WECS with its connectivity to grid has been developed.
- Two new control schemes for WECS have been developed.
    - One control scheme operates through indirect current control on regulation of frequency and terminal voltage of the DFIG insensitive to any parametric variations of machine and load dynamics. In addition to this the control offers flexibility in power exchange through rotor circuit at unity power factor with very low THD.

- The second control scheme operates on decoupling of active and reactive power. The current control forces the DFIG to follow the reference power inputs and in a way can extract maximum power from the wind turbine.

- Simulated results with two new control schemes have clearly demonstrated that both schemes operate very close to desired conditions and are insensitive to any parametric variations of machine and load dynamics.
- It is also demonstrated that control scheme responds fast during transient conditions and work well under varying wind conditions.

5.3 Suggestions for future work

- The laboratory prototype of these systems may be developed to validate the design, model and control techniques.
- These control schemes can be practically implemented with the help of DSP microcontrollers. Sensor reduction can be envisaged with proposed control techniques for DFIG.
- In present work the stator losses are minimized, the control technique may be further be developed to minimize the losses both in stator and rotor circuits.
- The proposed technique could be applied to isolated systems. The proposed techniques may further be developed to incorporate hybrid system i.e., isolated WECS with fuel cell, photovoltaic cell, diesel generator etc.